

# A fire modeling approach to assess wildfire exposure of valued resources in central Navarra, Spain

Fermín J. Alcasena<sup>1,2</sup> · Michele Salis<sup>2,3</sup> · Cristina Vega-García<sup>1</sup>

Received: 25 April 2015/Revised: 23 August 2015/Accepted: 15 October 2015/Published online: 27 October 2015  
© The Author(s) 2015. This article is published with open access at Springerlink.com

**Abstract** Wildfires are a growing threat to socioeconomic and natural resources in the wildland–rural–urban intermix in central Navarra (Spain), where recent fast-spreading and spotting short fire events have overwhelmed suppression capabilities. A fire simulation modeling approach based on the minimum travel time algorithm was used to analyze the wildfire exposure of highly valued resources and assets (HVRAs) in a 28,000 ha area. We replicated 30,000 fires at fine resolution (20 m), based on wildfire season and recent fire weather and moisture conditions, historical ignition patterns and spatially explicit canopy fuels derived from low-density airborne light detection and ranging (LiDAR). Detailed maps of simulated fire likelihood, fire intensity and fire size were used to assess spatial patterns of HVRA exposure to fire and to analyze large fire initiation and spread through source-sink ratio and fire potential index. Crown fire activity was estimated and used to identify potential spotting-emission hazardous stands. The results revealed considerable variation in fire risk causative factors among and within HVRAs. Exposure levels across HVRAs were mainly related to the combined effects of anthropic ignition

locations, fuels, topography and weather conditions. We discuss the potential of fire management strategies such as prioritizing mitigation treatment and fire ignition prevention monitoring, informed by fine-scale geospatial quantitative risk assessment outcomes.

**Keywords** Wildfire risk · Wildfire simulation · Highly valued resources and assets · Mediterranean areas · Forest–rural–urban intermix

## Introduction

Fuel load and continuity increased notably in southern Europe during the second half of the twentieth century due to fire exclusion policies, abandonment of marginal agricultural land, active conifer reforestation and reduced anthropic pressure on natural resources, mainly through firewood cutting and livestock grazing (Scarascia-Mugnozza et al. 2000; Loepfe et al. 2010; San-Roman-Sanz et al. 2013). Many mature forests are now dominated by a shrubby ladder fuel understory, and herbaceous pastures are being replaced by shrubby vegetation and young thickets (Lloret et al. 2002; Romero-Calcerrada and Perry 2004; Mouillot et al. 2005), which lead to more intense wildfires (Moreira et al. 2011). Changes in fuel load and continuity have been especially noticeable in areas around the northern rim of the Mediterranean basin, such as the pre-Pyrenees and the central Iberian Peninsula (Roura-Pascual et al. 2005; Vega-García and Chuvieco 2006). In these areas, larger wildfires now threaten many rural–urban interfaces and ecosystems adapted to frequent and low-intensity fire regimes (Pausas et al. 2004; Fulé et al. 2008). For instance, the 1998 Solsones wildfire in the central Catalanian pre-Pyrenees burned more than 20,000 ha

---

Handling Editor: Dr. Martin Moog.

✉ Fermín J. Alcasena  
ferminalcasena@eagrof.udl.cat

<sup>1</sup> Agriculture and Forest Engineering Department (EAGROF), University of Lleida, Alcalde Rovira Roure 191, 25198 Lleida, Spain

<sup>2</sup> IAFES Division, Euro-Mediterranean Center on Climate Change (CMCC), Via De Nicola 9, 07100 Sassari, Italy

<sup>3</sup> Department of Science for Nature and Environmental Resources (DIPNET), University of Sassari, Via De Nicola 9, 07100 Sassari, Italy

where the previous largest fire events in that area burned few hundred hectares. Moreover, recent studies in the Mediterranean basin have highlighted that climate change projections suggest increasingly long and frequent heat waves and greatly reduced summer precipitation (Gao and Giorgi 2008; Giorgi and Lionello 2008; Giannakopoulos et al. 2009; Arca et al. 2012), which are consistent with observed trends (Pal et al. 2004; Cardil et al. 2013a). This weather scenario will likely increase wildfire season duration and the frequency of weather conditions associated with large fire events (IPCC 2014).

Annually, some 51,200 forest fires burn approximately 477,400 ha in southern European countries (from 1980 to 2013, in Portugal, Spain, France, Italy and Greece; Rodriguez-Aseretto et al. 2014) and over 85 % of fires are caused by anthropic activities (San-Miguel-Ayanz and Camia 2010). A small number of large catastrophic fire events are responsible for most of the burned area (Ganteaume et al. 2013; San-Miguel-Ayanz et al. 2013) and greatest loss of highly valued resources and assets (HVRAs). These fires overwhelm fire suppression capabilities despite the fact that suppression resource levels and fire crew training are better than ever before (WWF 2006, Cardil et al. 2013b). In recent years, not only in the USA, Canada or Australia but also in the Mediterranean basin, extreme fire behavior events have exhibited fire-line intensities, spreading and massive spotting (Koo et al. 2010; Molina et al. 2010) that have made them resistant to suppression efforts until a change in weather (i.e., wind speed reduction and relative humidity increase) or in fuel load and continuity (Finney 2007; Werth et al. 2011). These events have challenged fire risk management activities and policies and revealed the need to integrate fire risk mitigation into landscape management actions, through fire ignition prevention plans and strategies to reduce fuel load and continuity (Fernandes et al. 2013). Most previous attempts to implement landscape fire management and planning in the EU have led to coarse scales and static, non-quantitative assessment outcomes of limited utility for landscape fire managers (reviewed in Miller and Ager 2013). Nevertheless, recent studies based on quantitative fire modeling assessment frameworks have been developed for the southern EU at various scales (Kalabokidis et al. 2013; Salis et al. 2013; Mitsopoulos et al. 2014; Alcasena et al. 2015), as well as for the USA (Ager et al. 2014a; Thompson et al. 2012, 2015).

Fire modeling approaches that account for site-specific key drivers of wildfire spread can provide reliable burned area estimates, particularly where large wildfires are responsible for most of the burned area (Calkin et al. 2011; Miller and Ager 2013). In the Mediterranean areas, fire ignition location alone is a poor estimator of burned area,

but fire spread modeling must account for historical ignition occurrence since anthropic activities are responsible for spatial-temporal ignition patterns (Bar-Massada et al. 2011; Ager et al. 2014b; Salis et al. 2014, 2015). Wildfires can be accurately and massively replicated using fire modeling programs such as FlamMap, FSim or Randig (Finney 2006), which are built on the computationally feasible and efficient minimum travel time (MTT) fire spread algorithm (Finney 2002). It has been extensively demonstrated in previous studies that MTT can accurately predict fire spread and replicate large fire boundaries for heterogeneous landscapes in the USA (Ager et al. 2010a, 2012) and the southern EU (Salis et al. 2013; Kalabokidis et al. 2013; Alcasena et al. 2015). MTT has been used for diverse purposes, such as endangered species habitat loss assessment (Ager et al. 2007), municipal watershed wildfire exposure assessment (Scott et al. 2012), urban planning (Haas et al. 2013), measurement of the effects of fuel treatments on forest carbon (Ager et al. 2010b) and landscape-level fuel treatment optimization (Finney 2007; Finney et al. 2007; Chung et al. 2013). Nevertheless, when used under different conditions to those in which the simulators were developed, accurate fire spread model calibration and input data validation are needed to generate reliable results (Arca et al. 2007; Salis 2008).

Advances in laser imaging detection and ranging (LiDAR) remote sensing technologies have facilitated the creation of high-resolution spatially explicit maps of canopy fuel metrics (i.e., canopy cover, canopy height, canopy base height and canopy bulk density; Scott and Reinhardt 2001), which improve these input metrics for wildfire behavior modeling (Andersen et al. 2005; Erdody and Moskal 2010; García et al. 2011; Gonzalez-Olabarria et al. 2012a; Hermosilla et al. 2014). Other remote sensing technologies such as near-infrared aerial imagery have been also used for fuel model mapping (Fallowski et al. 2005; Arroyo et al. 2008), but only small-footprint discrete-return airborne LiDAR pulses can penetrate beneath the tree canopies to allow pixel-based reconstruction of three-dimensional forest structure characteristics for large regions. Canopy fuel metrics can be estimated from LiDAR point cloud statistically derived regression models and processed at broad scales using analytical tools (Mc Gaughey 2014). Previous studies have suggested that the use of LiDAR canopy fuel metrics as input data could allow for more realistic predictions of fire spread and intensity (Mutlu et al. 2008), particularly in crown fire modeling (Peterson and Nelson 2011). In most previous studies, however, canopy fuel metrics have been derived from low-resolution layers and expensive field surveys, where pixel data are spatially homogeneous within stands or fuel models. Current efforts to increase LiDAR data

availability for large areas, such as the PNOA project (*Plan Nacional de Ortofotografía Aérea*; Ministerio de Fomento 2010), which provides low-density ( $0.5 \text{ first returns m}^{-2}$ ) airborne LiDAR data for the whole of Spain, permit the estimation of pixel-based canopy fuel characteristics (González-Ferreiro et al. 2014) and are invaluable resources for fire managers, as this study demonstrates.

Beyond fire modeling, fire risk is defined as the expected loss or benefit to any number of socioecological values affected by fire, and its calculation requires an understanding of the spatially explicit burning likelihood and the value change in resources from fire intensity (Finney 2005). Consequently, quantitative fire risk assessment must encompass three major elements: (1) estimation of the spatially explicit fire likelihood and intensity across the territory; (2) geospatial identification of the HVRAs that could undergo a change in value due to wildfire; and (3) estimation of this change in value change in response to fire (Thompson et al. 2011; Miller and Ager 2013; Scott et al. 2013). By contrast, wildfire exposure analysis requires the geospatial overlapping of the causative risk factors with the location of each HVRA, and although it does not explicitly consider the potential impacts of fire (Miller and Ager 2013), it is more than adequate for wildfire risk assessments (Ager et al. 2012; Salis et al. 2013; Kalabokidis et al. 2013) and mitigation planning (Ager et al. 2010a). Fire effects on HVRAs have been analyzed in integrated fire risk assessment frameworks through the use of expert appraisals of fire intensity versus net value change response functions (Calkin et al. 2011; Thompson et al. 2012), but the difficulty of distinguishing between low-likelihood high-hazard events and high-likelihood low-intensity events can critically undermine risk assessment and mitigation planning.

The goal of this study was the methodological implementation of an improved fine-scale quantitative wildfire exposure assessment for HVRAs, as well as the identification of the likely areas of large fire initiation and spread, to better inform landscape-level fire management in a forest–rural–urban intermix area in central Navarra (Spain). Our approach integrates a pixel-based LiDAR canopy fuel characterization that uses the MTT algorithm to model burn probability (fire likelihood estimate; Ager et al. 2010a), conditional flame length (fire intensity estimate; Scott et al. 2013) and fire size (Calkin et al. 2011; Ager et al. 2012) fire risk causative factors affecting HVRAs. We also performed complementary analyses of likely large fire initiation areas using the fire potential index (Salis et al. 2013), large fire transmission using the source-sink ratio (Ager et al. 2012) and likely active torching and ember-emitting stands based on active crown fire probability.

## Materials and methods

### Study area

The study area is located in the northern-rim Mediterranean area of the Pamplona Basin (Autonomous Community of Navarra, Spain) and encompasses a rectangular frame of 28,000 ha (Fig. 1). The study area is limited by the regional capital Pamplona to the southwest, where most of the population lives (in Pamplona and the neighboring towns, with a total of  $\sim 250,000$  inhabitants; [www.navarra.es](http://www.navarra.es)), while the central and northern parts present a very low population density and a highly scattered rural–urban intermix, characterized by sparsely distributed small villages with fewer than 150 inhabitants.

The orography consists of open and flat areas in the southern part in contrast with rough mountainous terrain in the northern part, ranging from 375 m in the south to highest peaks of 1100 m in the north (Fig. 1). Most watersheds present small watercourses that flow predominantly to the south to converge at the Arga River. The climate is transitional Mediterranean in lower elevations to temperate in the mountains, with cool summers and abundant precipitation, though with two dry months. The average annual rainfall of  $\sim 900$  mm is evenly distributed from autumn to spring, and water shortages occur from July to mid-September. The mean annual temperature is  $\sim 12$  °C, ranging from  $\sim 6$  °C in the coldest month to  $\sim 21$  °C in the warmest month, but easily peaks above 35 °C on summer days. The average wind speed in summer is moderate ( $21.6 \pm 10.8 \text{ km h}^{-1}$ ), and the most frequent wind direction is NW–N, with southerly wind less frequent but also common (<http://meteo.navarra.es>).

The vegetation in the study area (Fig. 2) corresponds to *Roso arvensis-Quercetum humilis* phytosociological vegetation series (Peralta 2000). Pine forests occupy a sizeable proportion of the area (11.3 %), consisting of *P. nigra* ssp. *austriaca* Endl. afforestations in marginal agricultural lands and *P. sylvestris* L. natural forests in the northeastern mountains. Broadleaf Mediterranean oak woodlands (18.4 %) occupy south-facing slopes, while *Q. pubescens* Willd. are found at mid-high altitudes and *Q. ilex* L. at low altitudes. Some north-facing slopes in the northern mountains are occupied by mature *Fagus sylvatica* L. stands (5.4 %). Shrubby pastures are a patchy mosaic of *Juniperus communis* L., *Rosa canina* L., *Echinopartum horridum* (Vahl.) Rothm. and *Prunus spinosa* L. formations (10.6 %), which intermingle with, or are replaced by, *Genista scorpius* (L.) DC., *Thymus vulgaris* L. and *Quercus coccifera* L. in shallow soils and rocky areas (0.2 %).

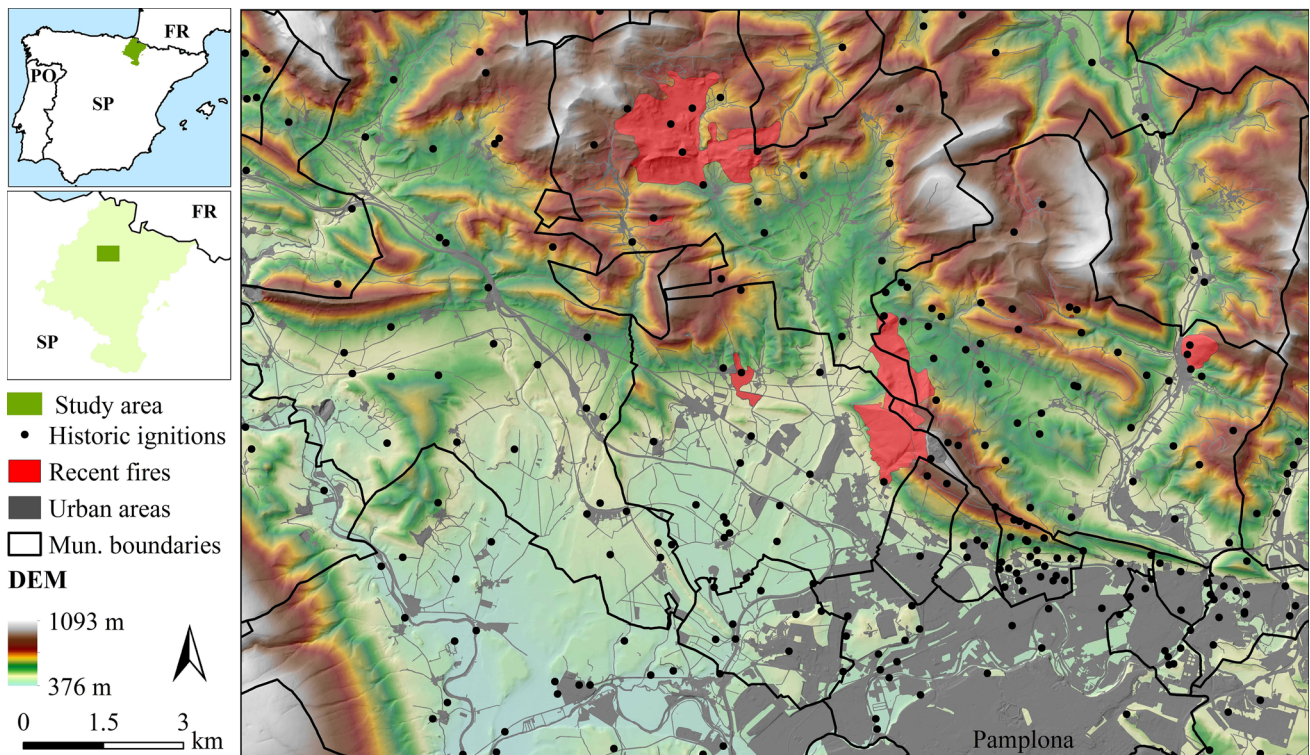


**Fig. 1** Map of elevation, urban areas, historical ignitions (20 years, data for 1985–2012; EGIF, MARM 2012), recent fires (2000–2012; Government of Navarra pers. comm., 2012), and municipal

boundaries in the study area (28,000 ha), located in central Navarra (northern Spain). The municipality of Pamplona is located in the southeastern of the study area

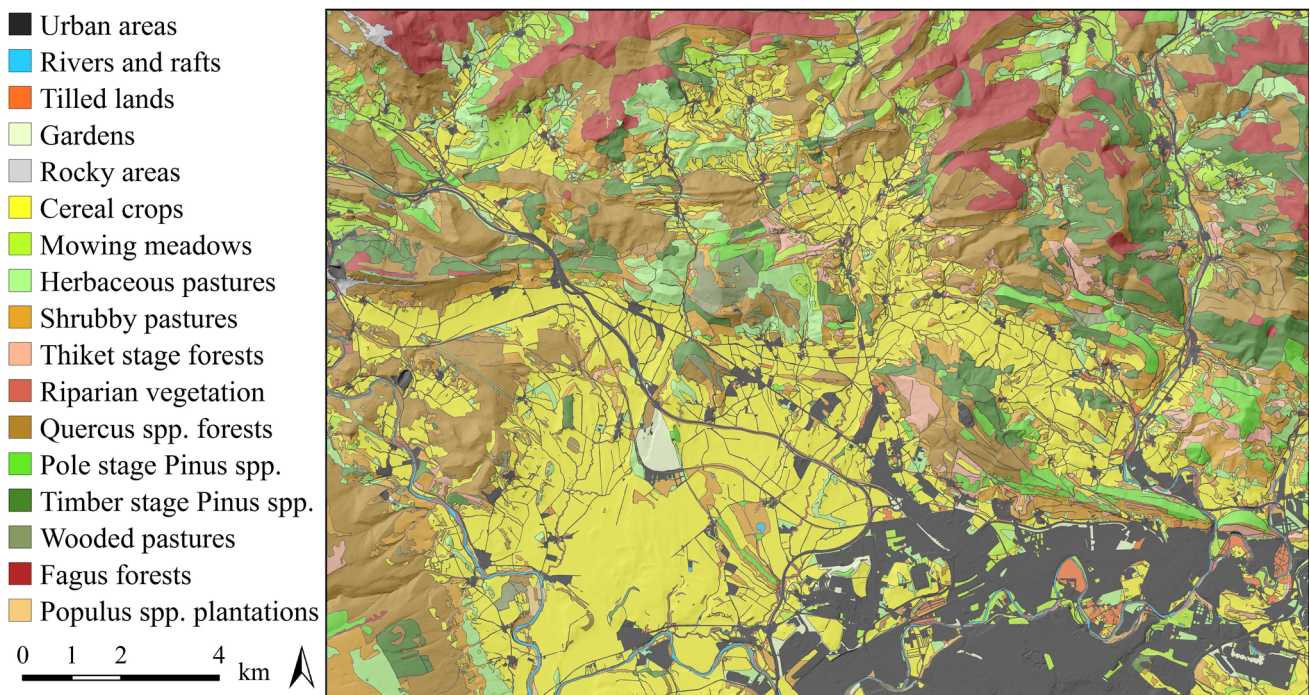


**Fig. 2** Map of the vegetation types in the study area, derived from the SIGPAC 2014 (<http://sigpac.navarra.es>) and the 2012 Crops and Land Use Map (<http://idena.navarra.es>) themes for fuel model assignments

Riparian vegetation is restricted to the major watercourses where *Populus nigra* L., *Fraxinus angustifolia* Vahl. and *Salix atrocinerea* Brot. predominate, with a dense and closed shrubby *Rubus fruticosus* L. stratum (0.5 %). Natural herbaceous Meso-xerophytic pastures (e.g., *Brachypodium pinnatum* L., *Bromus erectus* Huds. and *Trifolium pratense* L.) cover transitional areas between forests and cultivated lands (6.3 %) and are usually managed as extensive livestock-grazing areas. Rainfed cereal crops (i.e., *Triticum aestivum* L., *Hordeum vulgare* L. and *Avena sativa* L.) occupy the valley bottom and areas suited to mechanization (26.1 %), whereas in the wetter northern areas, cereal crops are replaced by hay meadows (4.1 %; e.g., *Lolium perenne* L., *Agrostis capillaris* L. and *Arrhenatherum elatius* (L.) Beauv.). Urban developments, which are mainly concentrated in the southwestern part of the study area, occupy 13.7 % of the land. Land ownership is highly fragmented, and forest areas are mainly public and owned by the corresponding authorities. Local authorities are responsible for forest management under the supervision of the regional forest service.

### Wildfire history

The study area is one of the most hazardous and fire-prone regions in the Autonomous Community of Navarra, both in terms of fire number and annual burned area (0.046 fires  $\text{km}^{-2} \text{year}^{-1}$  and 0.2 % of surface burned  $\text{year}^{-1}$  on average; MAGRAMA 2014), with simultaneous episodes that have overcome fire suppression capabilities and threatened HVRAs in recent years (e.g., Juslapeña and Izagaondoa wildfires in 2009). Small fires (<10 ha) account for only 10 % of the overall burned area despite constituting 94 % of the fire number, whereas the less frequent large fires (>100 ha, and 1.3 % in fire number) are responsible for 56 % of the burned area; no fires larger than 1000 ha have been reported in the database period (Spanish EGIF database 1985–2012, MAGRAMA 2014; Fig. 3a). The wildfire season usually falls between July and September and is responsible for 86 % of the burned area recorded over the study period; it is followed by a less severe late-winter/spring season (Fig. 3b). Large inter-annual variability in burned area has been also reported, due to differences in weather and fuel moisture conditions during wildfire seasons: The largest burned areas were reported in 1991, 2005 and 2009. Although the causes of many fires in the study area are still unknown, the main known causes of fire ignitions are (Fig. 3c): agro-pastoral burning (20 %), arson (12 %), engines and machines (3 %), railways (3 %), power lines (2 %) and lightning (2 %).

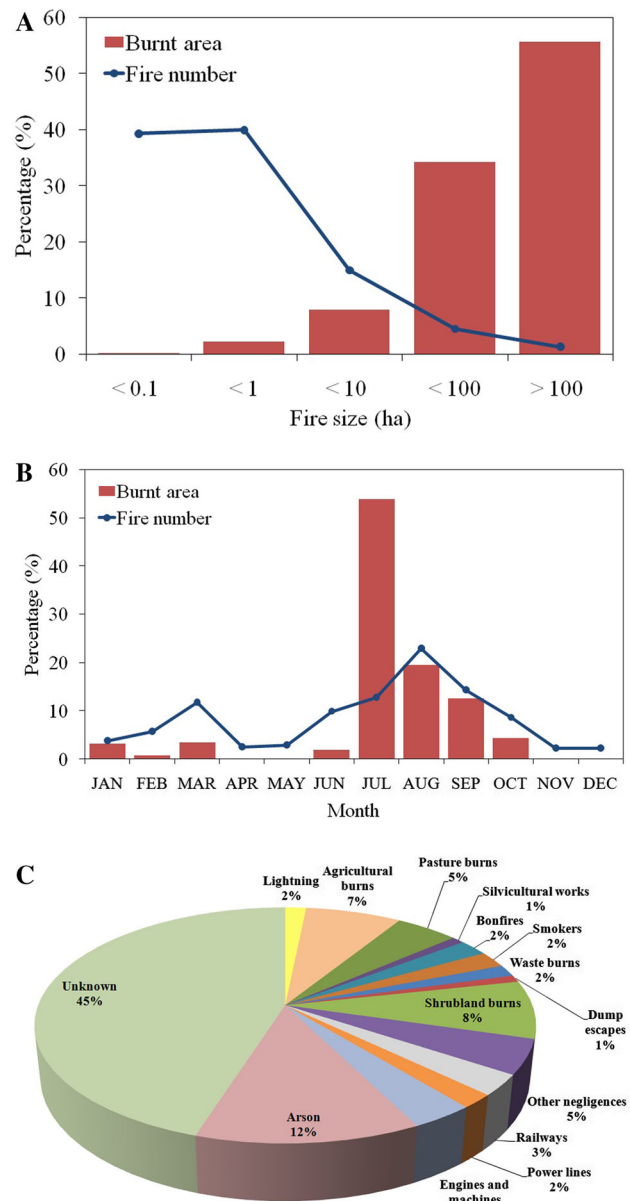


**Fig. 3** Wildfire history. Burned area and fire number by fire size category (a), monthly frequency distribution (b) and fire ignition causes (c) in the study area in central Navarra (Spain), from the period 1985–2012 (MAGRAMA 2014)

### Input data for fire spread and behavior modeling

Fuel model input data (i.e., surface fuels and canopy fuel characteristics) and topography (i.e., aspect, elevation and slope) input data layers were assembled in a 20-m-resolution landscape file (.LCP), as required by FlamMap (Finney 2006), using ArcFuels 10 (Ager et al. 2011). The surface fuel map was derived from the land use/land cover typologies of the 1:5000 scale Agricultural Plots GIS shapefiles (SIGPAC, <http://sigpac.navarra.es>; Gobierno de

Navarra 2014a), where herbaceous, shrubby and forest land cover formations are accurately delimited. Patches classed as forested in SIGPAC without further specification were classified in fuel types using the Government of Navarra's Crops and Land Use Map (*Mapa de Cultivos y Aprovechamientos*, <http://idena.navarra.es>; Gobierno de Navarra 2014b), in which forest types are classified according to tree stand species composition and developmental stage (Table 1; Fig. 2). Standard fuel models (Scott and Burgan 2005; Fernandes 2009) were assigned to the land use/land cover types (Table 1) to obtain the surface fuel map of the study area (Fig. 2). Spatially explicit canopy fuel characteristics (i.e., canopy cover, canopy bulk density, canopy base height and canopy height) were obtained at 20-m resolution from low-density (0.56 returns  $m^{-2}$ ) airborne LIDAR data (Gobierno de Navarra 2014c), with models from other studies (Gonzalez-Olabarria et al. 2012a) using Fusion software (Mc Gaughey 2014). The LIDAR flight was carried out under the supervision of the Government of Navarra in 2011–2012 by TRACASA S.A. using a Leica ASL60 sensor with a pulse repetition rate of 97 kHz, a scan frequency of 37.5 Hz, a maximum scan angle of 40° and an average flying height of 3315 m (Gobierno de Navarra 2014c); the results were integrated into the PNOA project (Ministerio de Fomento 2010). Elevation, slope and aspect input data were obtained from

5-m-resolution digital elevation map from the National Geographic Institute (IGN, [ign.es](http://ign.es); Ministerio de Fomento 2010).

Wind speed and direction for fire modeling were determined from wildfire season data recorded at the Airport of Noain, at the standard height reference of 10 m (July–September, 1998–2013; AEMET pers. comm. 2014), at which wind data are considered representative for the study area and are not influenced by topography. Two dominant wind directions (43 % northwest and 21 % north; Fig. 4) were most frequent during the wildfire seasons, with south winds also recorded (15 %; Fig. 4). We set as a modeling reference the 97th percentile of wind speed for every wind direction during the wildfire season (Fig. 4). In order to obtain more realistic wind field input data to inform wildfire simulations, we used a mass-consistent model (WindNinja; Forthofer et al. 2014a, b) to generate 50 m resolution wind field grids, considering 12 wind speed and direction scenarios (Table 3). WindNinja computes spatially varying wind fields from elevation, a domain-mean initial wind speed and direction, and specification of the dominant vegetation data in the area (Forthofer and Butler 2007).

The information on dead fuel moisture emulated the conditions of the Izagaondoa 2009 wildfire, which was the default choice for replicating extreme wildfire conditions in

**Table 1** Vegetation types and respective fuel models and fuel moisture contents used for wildfire simulations. Dead fuel moisture contents were associated at recent extreme fire events and live

woody fuel moisture content, as well as crown foliar moisture content (85 %) where derived from bibliography (Chuvieco et al. 2011). *na* not applicable

Vegetation type	Incidence (%)	Fuel model	1-h fuel (%)	10-h fuel (%)	100-h fuel (%)	Live herb. fuel (%)	Live woody fuel (%)
Urban areas and development	13.7	NB1 (Scott and Burgan 2005)	na	na	na	na	na
Rivers and rafts	0.7	NB8 (Scott and Burgan 2005)	na	na	na	na	na
Orchards, tilled lands	0.9	NB3 (Scott and Burgan 2005)	na	na	na	na	na
Gardens and golf courses	0.7	GR1 (Scott and Burgan 2005)	11	13	15	100	100
Rocky areas	0.2	GS1 (Scott and Burgan 2005)	6	8	10	50	55
Cereal crops	26.1	GR5 (Scott and Burgan 2005)	6	8	10	40	55
Mowing hay meadows and grazed pastures	4.1	GR2 (Scott and Burgan 2005)	6	8	10	40	55
Herbaceous pastures	6.3	GR4 (Scott and Burgan 2005)	6	8	10	40	55
Shrubby herbaceous pastures	10.3	SH6 (Scott and Burgan 2005)	6	8	10	50	60
Thicket-stage forests and shrublands	1.9	SH5 (Scott and Burgan 2005)	6	8	11	60	80
Riparian vegetation	0.5	SH8 (Scott and Burgan 2005)	6	8	11	60	85
<i>Quercus</i> spp. forests	18.4	TU3 (Scott and Burgan 2005)	7	9	11	60	80
Pole-stage <i>Pinus</i> spp. plantations	2.7	PCL (Fernandes 2009)	7	9	11	60	75
Timber-stage <i>Pinus</i> spp. plantations	6.7	SH3 (Scott and Burgan 2005)	7	9	11	60	75
Wooded pastures	0.9	GR3 (Scott and Burgan 2005)	7	9	11	60	80
Timber-stage <i>Populus</i> spp. plantations	0.1	SH3 (Scott and Burgan 2005)	8	11	14	60	80
<i>Fagus</i> spp. Forests	5.4	TL2 (Scott and Burgan 2005)	9	11	14	60	85

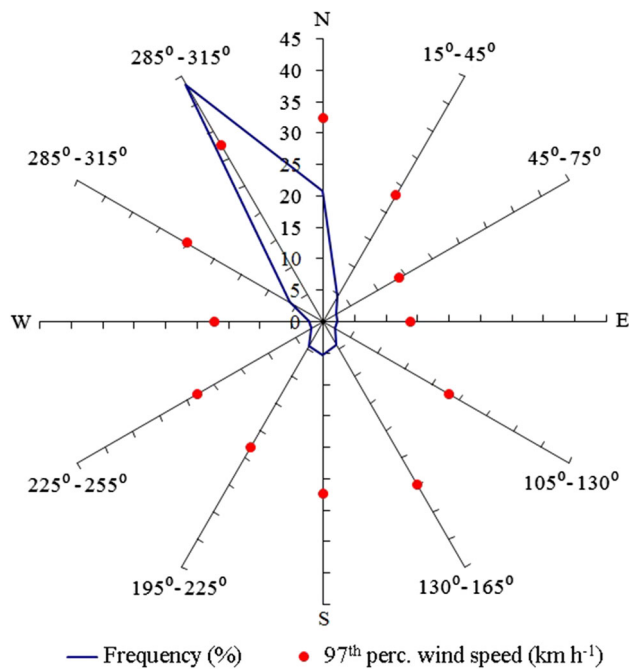


**Fig. 4** Wind direction frequency and 97th percentile wind speed ( $\text{km h}^{-1}$ ) rose for the July–September wildfire season (data from the period 1998–2013; AEMET pers. comm. 2014)

central Navarra (Fire Service of Navarra pers. comm. 2013). Live woody fuel moisture content for surface fire spread and foliar moisture content for crown fuels were also selected, in agreement with species and vegetation-complex data derived from sampling campaigns conducted in Spain in recent years (Chuvienco et al. 2011). We considered the observed 97th percentile values of the annual fuel moisture records, to take into account the conditions most frequently associated with the peak wildfire season (Table 1).

In order to replicate the observed fire ignition spatial pattern (most ignitions occur close to main roads and urban developments; Fig. 1), we used the historical fire ignition coordinates (ADIF database 1985–2012; MAGRAMA 2014) for the study area to create an input file of 2500 historical ignition points for fire modeling. Initially, a kernel-smoothed point density grid was constructed from the observed ignition locations (Gonzalez-Olabarria et al. 2012b), with a bandwidth (search radius) of 1000 m; it was then divided by the number of years in the fire record to create an historical ignition probability (IP) grid, and the 2500 fire ignition points were drawn (Kalabokidis et al. 2013; Salis et al. 2013; Alcasena et al. 2015).

### Wildfire simulations

Fires were simulated using the MTT fire spread algorithm (Finney 2002) as implemented in FlamMap 5 (Finney 2006), which requires geospatial input data on topography

and fuels, as well as data on weather, fuel moisture content and fuel characteristics. The algorithm finds the straight-line shortest path between the nodes in a fire-front network, producing spatial data fields of arrival time (and other characteristics) recorded at discrete points (Finney 2006). Surface fire spread is predicted by the semiempirical Rothermel equation (Rothermel 1972), and crown fire initiation is evaluated according to Van Wagner (1977), as implemented by Scott and Reinhardt (2001). FlamMap assumes constant wind speed and direction within every pixel as defined in the wind grid, and constant fuel moisture content. It is therefore suitable for simulating short-duration fire events (Ager et al. 2011) like those recorded in the study area.

To calibrate the fire spread model and validate the standard fuel models assigned, we attempted to replicate the perimeter of the Izagaondoa wildfire, which started with the reactivation of a fire caused by lightning the previous day. It burned 873 ha (Gobierno de Navarra pers. comm. 2013) in 4.5 h of active spread on July 22, 2009 (Fire Service of Navarra, pers. comm. 2013). Fire crews worked mostly on the fire flanks and rear, but no data were available to account for the influence of suppression efforts on the final burned area. The fire developed under strong southern winds of over  $40 \text{ km h}^{-1}$ , low atmospheric relative humidity (under 15 %) and with several spotting fires, leading to an average rate of spread above  $20 \text{ m min}^{-1}$  (Fire Service of Navarra, pers. comm. 2013). Multiple simulations were run (10 simulations at 10 m resolution) to analyze the agreement between observed and simulated perimeters, since the predicted burned area changes from simulation to simulation due to the stochastic behavior caused by spot fires in any run (Cochrane et al. 2012), although all input data and parameters were kept constant (Fig. 5). Simulation overestimation of backing and flanking fire spread areas was expected and observed, since suppression efforts that contained the fire spread in these areas were not considered in the model (in any case, containment activities have a very limited influence on heading fire spread during extreme fire events). The average simulation accuracy for the burned area, as measured by the Sorensen coefficient, was  $0.50 \pm 0.07$  (Legendre and Legendre 1998), yielding an overall accuracy of  $0.80 \pm 0.07$  (Congalton and Green 1999).

Twelve simulations were run, considering a set of wind scenarios (different wind directions and wind speeds), constant fuel moisture content and the 2500 historical fire ignitions (Table 3). Overall, 30,000 fires were simulated at 20-m resolution, with a 0.10 spot probability and a spread duration of 8 h. Simulated fires were large enough to burn the pixels more than 100 times on average and over 97 % of the burnable area at least once. The simulation outputs were burn probability (BP), conditional flame length

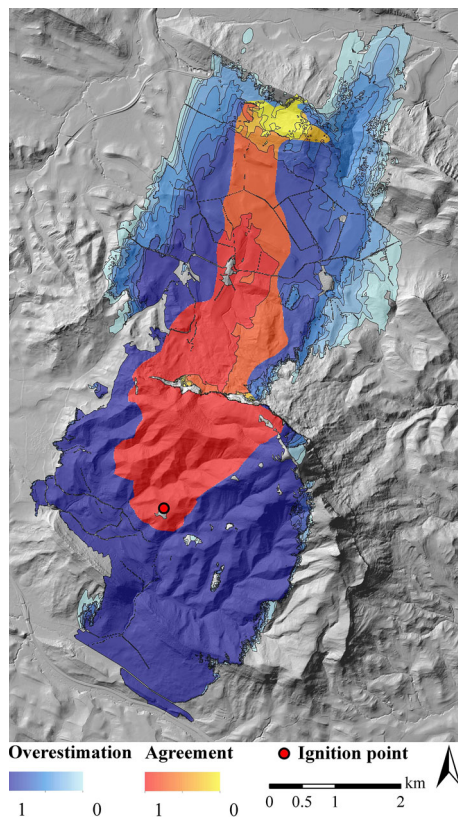


**Fig. 5** Degree of agreement (0 to 1, warm colors) and overestimation (0 to 1, cool colors) in the Izagaondoa fire (on July 22, 2009, 873 ha burned) replication considering the observed final perimeter (Gobierno de Navarra pers. comm. 2014). The real fire showed important spotting distances reaching 300 m. The FlamMap MTT simulation did not take into account the attempted suppression of backfire spread or flanking. The fire was simulated at 10 m resolution, using 50 m resolution gridded wind fields

(CFL), fire size (FS) and crown fire activity (CFA). Burn probability defines the number of times a pixel burns as a proportion of the total number of fires and is defined as follows:

$$BP_{xy} = \frac{F_{xy}}{n_{xy}} \quad (1)$$

where  $F_{xy}$  is the number of times the pixel  $xy$  burns and  $n_{xy}$  is the number of simulated fires. In other words, the burn probability for a given pixel is an estimate of the likelihood that the pixel will burn given a single fire ignition in the study area and the assumed fuel moisture and weather conditions (Ager et al. 2010a; Salis et al. 2013).

Wildfire intensity depends on the direction from which the fire reaches a pixel relative to the major direction of fire spread (i.e., heading, flanking or backing fire) and on slope and aspect (Finney 2002). FlamMap converts fire-line intensity (FI, in  $W m^{-1}$ ) to flame length (FL, in m) using Byram's (1959) equation:

$$FL = 0.0775 \times (FI)^{0.46} \quad (2)$$

Flame length distribution and BP were used to calculate the CFL for each pixel in the study area:

$$CFL = \sum_{i=1}^{20} \frac{BP_i}{BP} (FL_i) \quad (3)$$

where  $FL_i$  is the flame length (m; Eq. 2) midpoint of the  $i$ th category and BP is the burn probability (Eq. 1). For each pixel, FlamMap generates a frequency distribution of FL values (ranging from 0 to 10 m) that are divided into twenty 0.5-m fire intensity ranges. The CFL is the probability-weighted FL assigned to a fire and is a measure of wildfire hazard (Ager et al. 2010a). Flame length is a consistent fire property that embeds severity and spread rate (Scott 2006). We also analyzed FS outputs, which provide the coordinates of the ignition points and burned area (ha) of each fire.

The fire potential index (FPI; Salis et al. 2013) was used to identify the areas with a greater likelihood of an ignition that could lead to a large fire, since almost all ignitions (98 % in the study area; Fig. 3) are caused by anthropic activities. The FPI was calculated using the FS and the historical ignition locations:

$$FPI = FS \times IP \quad (4)$$

where FS is the average fire size for all fires that originated from a given pixel and IP is the historical ignition probability. The FPI combines the historical ignition point probability with simulation outputs of FS to measure the expected annual burned area for a given pixel under the assumed weather and fuel moisture conditions (Salis et al. 2013).

In addition, we used the source-sink ratio (SSR; Ager et al. 2012) to measure wildfire transmission through the landscape, calculated as:

$$SSR = \log \left( \frac{FS}{BP} \right) \quad (5)$$

where FS is the average fire size for all fires that originated from a given pixel and BP (Eq. 1) is the burn probability. The SSR measures a pixel's wildfire contribution to the surrounding landscape relative to the frequency with which it is burned by fires originated elsewhere or ignited in the pixel. If an ignition occurs, pixels with high BP values that do not generate large fires behave as wildfire sinks, whereas pixels with low BP but large FS behave as wildfire sources (Ager et al. 2012).

Crown fire activity was also modeled with FlamMap for all cells of the landscape containing a forest stand. To determine crown fire activity, the surface fire-line intensity is compared with the intensity threshold that is critical to involving the overlying crown fuels. Crown fire typology



(i.e., passive or active; Van Wagner 1977) is then determined from the rate of spread threshold for the current fire spread direction (Rothermel 1972). Using active crown fire and BP output grids, we identified those stands where active crown fire is likely to occur in the large fire event, through the active crown fire probability (ACP), calculated as:

$$ACP = ACF \times BP \quad (6)$$

where ACF is the active crown fire-type occurrence (a binary value, 0 absence or 1 presence) of a pixel and BP (Eq. 1) is the related burn probability. Active crown fire probability can give crucial information about which stands are potentially responsible for ember emissions that could lead to spot fires, as well as high fire intensity areas where HVRAs could suffer severe fire effects.

### Highly valued resources and assets

Wildfire simulation outcomes must be coupled with geospatial identification of the HVRAs whose value may be affected, in order to analyze the differences in wildfire exposure between HVRAs of different types and within patches or structures (Calkin et al. 2011). HVRAs are key social, economic and ecological resources which are exposed to wildfire effects (Thompson et al. 2011; Scott et al. 2013). In the current study, we focused our analysis on four major HVRA typologies (Table 2): urban development, infrastructure, natural habitats (92/43/CEE Directive, <http://ec.europa.eu>; European Community 1992) and forest resource values. Each type is broken down into several classes according to human presence, economic value and ecological value, using geospatial data themes (Table 2). We obtained the HVRA data themes from IDENA (<http://idena.navarra.es>; Gobierno de Navarra 2014b) and IGN ([www.ign.es](http://www.ign.es); Ministerio de Fomento 2010).

### Graphical and statistical analyses

The 12 simulation output results for of BP, CFL, FS and CFA were combined weighting from the modeled wind scenario frequency (Table 3) to create the maps for the whole study area. The FS maps were obtained by filling the spaces between the smoothed data for simulated fire ignitions with a nearest-neighbor interpolation procedure (Ager et al. 2010a, 2012). The fire potential index (Salis et al. 2013), source-sink ratio (Ager et al. 2012) and ACP were derived from the combined maps of fire risk causative factors, IP and ACF.

Box plots of the main descriptive statistics were built to analyze the variations among HVRA classes (Table 2) for the modeled causative risk factors (BP, CFL and FS). To

graphically assess the differences in wildfire exposure among and within HVRA units through scatter plots, we calculated the average causative risk factor values considering a 60 m buffer home ignition zone (HIZ; Cohen 2008) for the building structure classes and within feature patches for the land use/land cover and habitat designation classes (Table 2).

Additionally, we calculated the average BP and active crowning surface in forest stands to identify and compare the patches most likely to burn and emit embers in the event of an extreme wildfire in the study area. For these analyses, we used the standard fuel models for forested land cover (Table 4) and the current land registry property boundaries at 1:5000 scale (<https://catastro.navarra.es>; Gobierno de Navarra 2014b) in order to account for the implicit constraint of forest land ownership in the study area and its effect on the selection and implementation of wildfire management policies.

## Results

### Spatial variation of fire likelihood, fire intensity and fire size in the study area

Burn probability values produced a highly variable spatial pattern in the study area that ranged from a low of  $8.0 \times 10^{-4}$  to a high of 0.197 (Fig. 6c). The areas with the highest values (BP > 0.15) were located on the northern and northeastern edges of the highly urbanized periphery of Pamplona (Fig. 2), corresponding mainly to cereal crops, *Pinus nigra* afforestations and Mediterranean oak forests. The highest average BP in the study area by land use/land cover was obtained for cereal crops, pole-stage afforestations and thicket-stage forests and shrublands, with values of  $0.8 \times 10^{-1}$ ,  $0.7 \times 10^{-1}$  and  $0.65 \times 10^{-1}$ , respectively (Table 3). Sharp transitions have been observed on the border marked by the Arakil River (southwestern part of the study area), which created a large barrier, as well as in the most important infrastructure border lines (e.g., the north–south roadway in the eastern part), which contained the fires originated in the central part of the study area. Nevertheless, some areas with a high concentration of ignitions on the south-facing slopes of the San Cristobal mountain (the closest mountain to the southeastern urban area; Fig. 1) also contributed to the high BP values in the central area, even in southern-wind-driven fire scenarios (15 % frequency; Fig. 4). The lowest BP values were observed in the northern–northeastern beech forests (avg. BP =  $9.9 \times 10^{-3}$ ; Table 3), where very few ignitions occurred and few fires arrived from elsewhere, and in gardens (average BP =  $0.95 \times 10^{-2}$ ; Table 3) in urban areas where only a very small number of ignitions can burn

**Table 2** Description of the highly valued resources and assets (HVRAs) considered in the study. The HVRAs were grouped into four types according to human presence, economic value and ecological value (<http://idena.navarra.es>; [www.ign.es](http://www.ign.es))

HVRAs types	Classes (abbreviation)	Number of sites or patches	Average size (ha)	Total area (ha)
Urban development	Residential housing (RH)	2572	0.036	93.201
	Industrial buildings (IN)	186	0.380	70.693
	Livestock farm buildings (FA)	122	0.030	3.605
	Churches and hermitages (CH)	33	0.036	1.168
	Cemeteries (CE)	53	0.243	12.859
	Sports areas (SA)	30	0.160	4.800
	Petrol stations (PS)	2	0.033	0.066
Infrastructure	Power lines (PL)	925	0.020	18.670
	Communication sites (CS)	8	0.001	0.008
	Water treatment plants (WT)	3	3.448	10.463
Natural habitats (Directive 92/43/CEE)	Oro-Mediterranean heaths with gorse (MH)	20	39.901	789.02
	Xerothermophilous scrub on rock slopes (XS)	3	51.137	153.431
	<i>J. communis</i> scrub on calcareous grasslands (JS)	2	4.268	8.535
	Seminal natural dry grasslands (SG)	17	29.818	506.910
	Pseudo-steppe with grasses (PG)	3	84.222	252.666
	Mediterranean and thermophilous scree (TS)	1	1.456	1.456
	Chasmophytic vegetation on rocky slopes (CV)	2	6.860	13.719
	Medio-European limestone beech forests (MB)	22	54.658	1202.472
	Alluvial forests with <i>A. glutinosa</i> and <i>F. excelsior</i> (AF)	10	6.264	62.645
	<i>S. alba</i> and <i>P. alba</i> galleries (GA)	3	0.724	2.173
Forest values	Mediterranean sclerophyllous forests (SQ)	22	55.056	1211.23
	<i>Pinus</i> spp. commercial timber plantations (PI)	590	5.650	3333.370
	Firewood forests (FF)	776	8.553	6636.843
	Livestock-grazing natural pastures (GP)	976	4.049	3952.153
	<i>Populus</i> spp. plantations (PO)	10	2.418	24.180

individual plots. The urban areas in the southwestern part of the study area (Fig. 2) correspond to non-burnable fuels (e.g., paved areas) and therefore did not support fire spread.

Fire intensity values produced a complex mosaic pattern, ranging from 0.04 to 9.68 m (Fig. 6b). High-fuel-load models located in steep-sloping area showed the highest intensities (e.g., 90th percentile CFL = 7.33 in thicket-stage forests and shrublands; Table 3; Fig. 6b). On average, thicket-stage forests and shrublands, shrubby herbaceous pastures and cereal crops showed the highest intensities, with CFLs of 4.01, 2.63 and 2.53 m, respectively (Table 3). Nonetheless, riparian vegetation, shrubby pastures and pole-stage *Pinus* spp. afforestations also burned locally at high intensities (90th percentile CFL > 3 m; Table 3). The lowest intensities were observed in gardens, wooded pastures and broadleaf litter-type fuel models (i.e., beech forests) located on north-

facing slopes in the northern part of the study area, with average intensities lower than 0.4 m (Table 3). The sharpest transitions were observed in sudden continuity changes from high to low fuel load models, as well as in areas where the alignment of slope and winds that drives heading fire spread is disrupted (e.g., the top of mountain edges). Overall, CFL values were consistent with the observed intensities of recent fire events in the study area (i.e., Juslapeña 2009 wildfire). Fire intensity was not affected by apparent spatial changes in non-burnable surface fuel continuity, whereas burn probability was affected by the spatial pattern of major water courses and communication infrastructure (Fig. 6b vs. a).

Fire size values revealed a clearly identifiable area in the northern-central part of the study area with the largest FS potential, where ignited fires covered an area of more than 3200 ha (Fig. 6c). There is also a large area with high FS

**Table 3** Description of wildfire simulation parameters and associated values. The 12 wind scenario wind grids were generated with WindNinja from historical weather data for the wildfire season (Fig. 4)

Input data	Description												
Number of scenarios	12 scenarios												
Wind scenarios	Frequency (%)	5	3	2	2	4	5	4	2	2	6	44	21
	Direction (°)	30	60	90	120	150	180	210	240	270	300	330	360
	97th percentile speed (km h <sup>-1</sup> )	32	23	14	14	23	30	27	23	23	17	25	32
Fire ignitions per scenario	2500 historically based ignition points												
Surface fuels	Fuel model (Scott and Burgan 2005; Fernandes 2009) assignment derived from SIGPAC 2014 and Crops and Land Use Map 2012												
Crown fuel metrics	Derived from 0.56 point m <sup>-2</sup> LIDAR point cloud (Gonzalez-Olabarria et al. 2012a)												
Dead and live fuel moisture	Izagaondua 2009 wildfire conditions and observed 97th percentile moisture content (Chuvieco et al. 2011)												

**Table 4** Fire simulation average and 90th percentile values for the different vegetation types in the study area (Fig. 1) for diverse fire risk causative factors (Fig. 6a–c). Non-burnable vegetation types have been excluded

Vegetation type	90th percentile BP (m)	Mean BP (m)	90th percentile CFL (m)	Mean CFL (m)	90th percentile FS (ha)	Mean FS (ha)
Gardens	0.0359	0.0095	0.253	0.163	1315	360
Rocky areas	0.0210	0.0135	1.306	0.930	3057	1905
Cereal crops	0.1506	0.0800	2.972	2.526	3495	1966
Mowing hay meadows and grazed pastures	0.0430	0.0228	1.381	1.005	3609	1843
Herbaceous pastures	0.0900	0.0426	2.977	2.053	4167	1993
Shrubby herbaceous pastures	0.1334	0.0582	3.968	2.630	3484	1798
Thicket-stage forests and shrublands	0.1191	0.0649	7.326	4.014	3579	1613
Riparian vegetation	0.1496	0.0450	3.431	1.983	2732	1171
<i>Quercus</i> spp. forests	0.0702	0.0341	2.062	1.497	3191	1931
Pole-stage <i>Pinus</i> spp. plantations	0.1621	0.0700	3.146	2.406	2435	1232
Timber-stage <i>Pinus</i> spp. plantations	0.1166	0.0433	1.433	1.023	3006	1693
Wooded pastures	0.0830	0.0428	0.524	0.395	2839	1632
<i>Fagus</i> spp. forests	0.0272	0.0099	0.509	0.249	3224	1780
Timber-stage <i>Populus</i> spp. plantations	0.0739	0.0345	1.215	0.791	1448	728

values in the western part, where ignited fires surpassed 1000 ha. By contrast, the southern and southwestern parts produced hardly any large fires of more than 1000 ha. Cereal crops and herbaceous pastures were the vegetation types with the highest average FS values, with almost 2000 ha (Table 3); gardens and *Populus* spp. plantations had the lowest FS results (<1000 ha; Table 3). Thicket-stage forests and shrublands did not show high average FS values, although locally ignited fires surpassed 3500 ha FS (90th percentile CFL; Table 3). Analysis of FS by distribution frequency (Fig. 7) showed that the bulk of fires ignited from the historical ignition pattern (>60 % fires)

burned between 750 and 6000 ha, while small fires (0–175 ha FS class) account for only <5 % of fires.

### Fire potential index and source-sink ratio

The source-sink ratio map (Fig. 8a) was used to identify the sink areas (low SSR) in the northern part of the study area, which were mainly low-spreading broadleaf forests (predominantly beech forests), where fires encroach from neighboring areas, and wildfire sources (high SSR), which were mainly housing-urban development borders (generally with higher values in the northern boundaries) in the

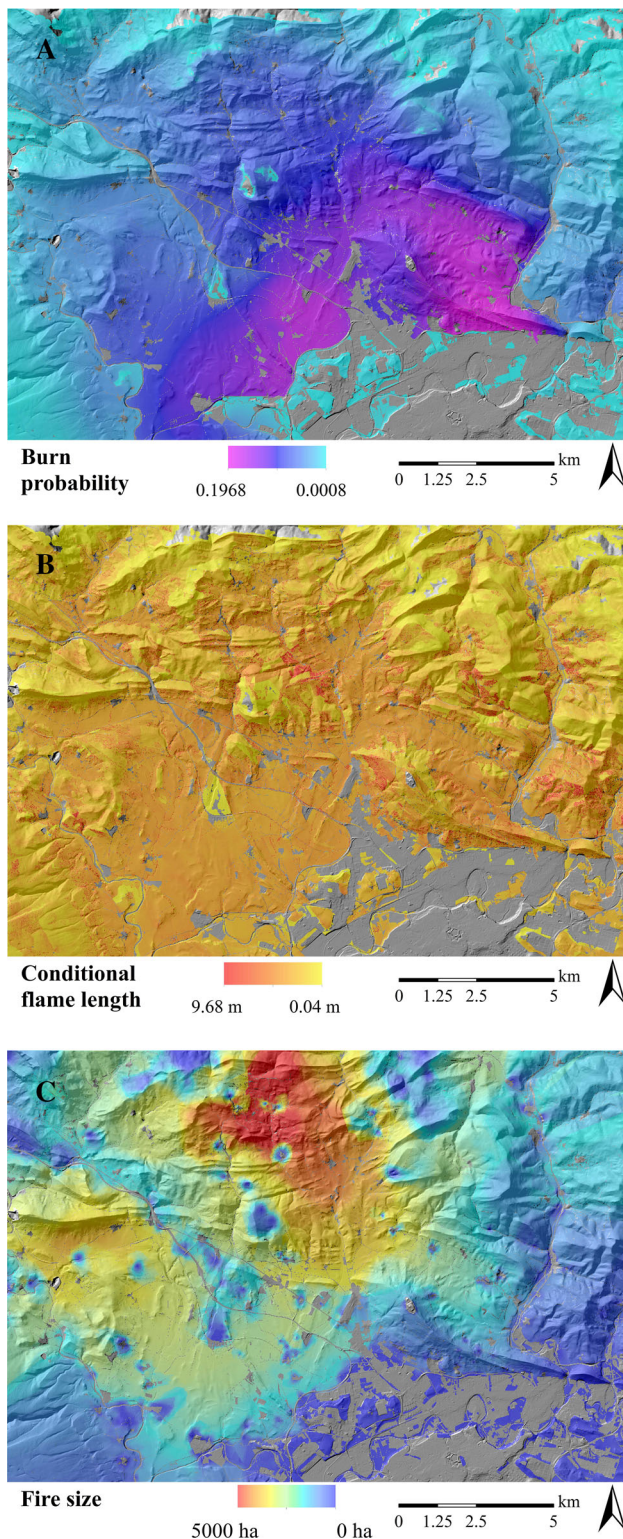


**Fig. 6** Fine resolution ( $20 \times 20$  m) maps of burn probability (a), conditional flame length (b) and kernel-smoothed fire size (c) for the study area. Non-burnable areas (paved and urban development, see Fig. 2) occupy large zones of the southwestern part of the study area

southern part of the study area and some forests in the central part with moderate FS and high burn probability values (Fig. 6a, c). In the case of the FPI, we clearly identified five major areas with the highest values, where the probability of an ignition leading into a large fire is very high with respect to the other areas (Fig. 8b). These areas were mainly located in the highest observed ignition point areas that also presented moderate-to-high FS values ( $FS > 2000$  ha; Fig. 6c). By contrast, mountainous areas on the eastern side of the study area showed the lowest FPI values, due to the lack of fire ignitions and low FS.

### Crown fire activity

Only a small proportion of the forested areas showed no torching (CFA; Fig. 9a); these were beech forests, managed old-grown *Pinus nigra* stands and grazed wooded pastures (Fig. 2). Nonetheless, although forest stands generally showed evidence of at least passive crown fires or isolated torching, our analysis identified active CFA patches in the study area (Fig. 9a), where fire spread (i.e., faster rates of spread than surface fire, as well as spotting) and intensity can easily overwhelm firefighting suppression capabilities (Andrews et al. 2011). The forest vegetation types presenting the highest incidence of CFA (Table 4) were pole-stage *Pinus nigra* afforestations (13.6 %), followed by Mediterranean oak forests (7.7 %) and timber-stage *Pinus nigra* afforestations (7.5 %). The results by fuel model type were in agreement with the observed CFA in recent fires (e.g., Juslapeña and Iza-gaondoa 2009).

In order to locate the stands that currently present the highest probabilities of ember emission under extreme wildfire conditions, we compiled the ACP map (Fig. 9b).

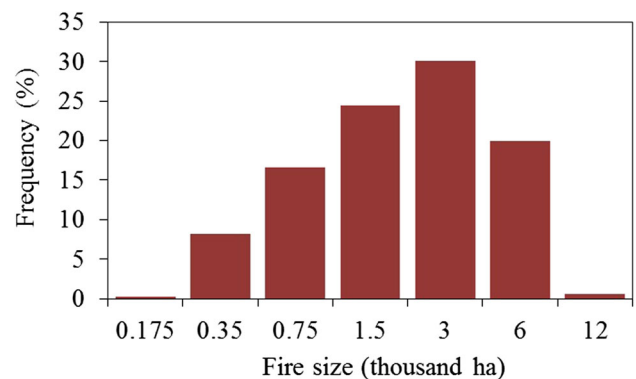


**Fig. 7** Frequency distribution of fire sizes in the study area from the simulation of 30,000 fires combining the 12 scenarios and using historical ignition patterns. Maximum fire size was 7265 ha

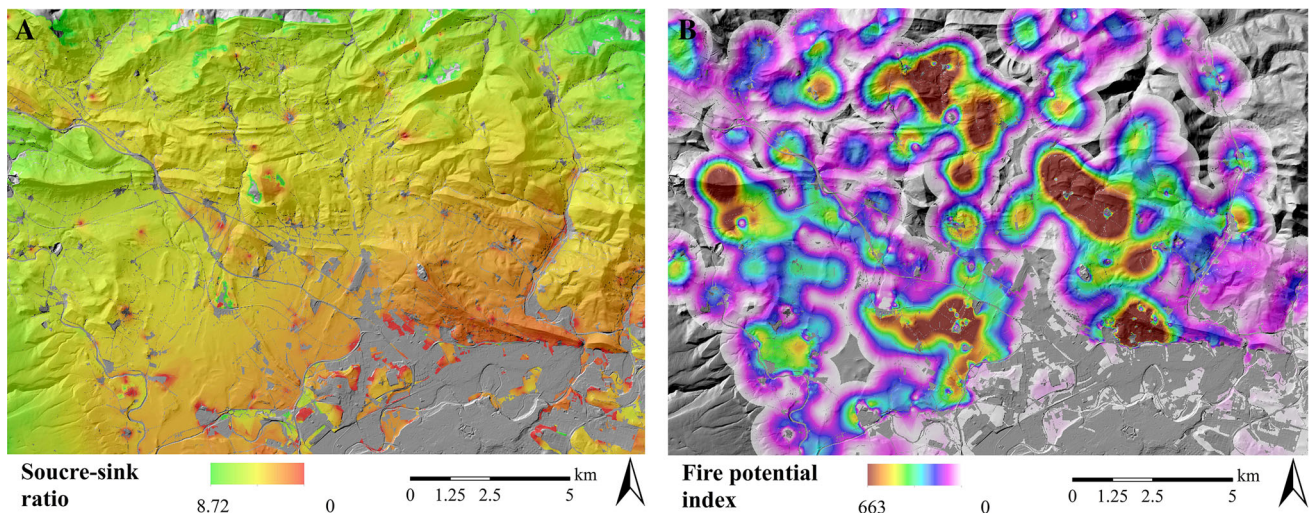


**Fig. 8** Map of source-sink ratio (b) and fire potential index (a) for the study area. Source-sink ratio (SSR) is a logarithm of the ratio between fire size (Fig. 6c) and burn probability (Fig. 6a), while the fire

potential index (FPI) was calculated from the historical ignition point density grid and the fire size map (Fig. 6c)

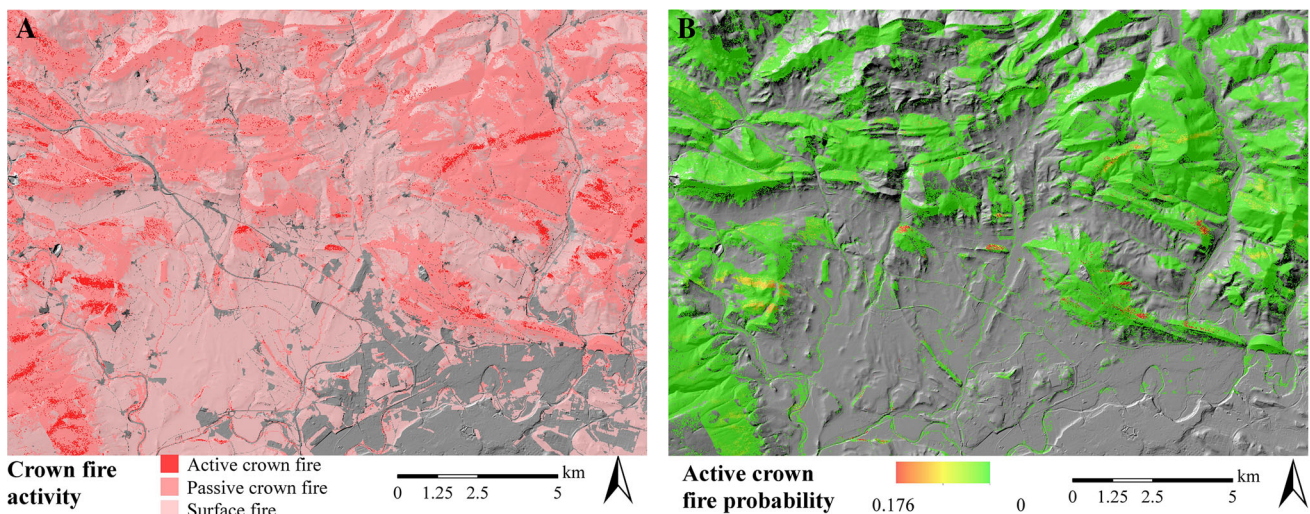


**Fig. 9** Crown fire activity (a) and active crowning probability (b) maps. The crown fire activity map shows the type of fire (surface fire, passive crown fire or active crown fire) and was used in

combination with the burn probability map (Fig. 6a) to identify the forest stands that, in case of a fire, would present crown fire activity and potential ember emission, as well as high post-fire mortality

The highest ACP values were recorded in small, unmanaged, closed and dense forest patches (<6 ha; Fig. 10) on north-facing mountain edges in the central part of the study area (Fig. 9b). Larger areas presenting CFA, mostly Mediterranean oak forests (>6 ha; Fig. 11), are located in the southwestern part of the study area (Fig. 9a), where BP values are four to five times lower than in the central part (Fig. 6a). In terms of ACP difference among active crown fire values, the highest values for patches in the central part of the study area with ACP > 0.10 decrease smoothly to ACP < 0.04 in the peripheral (southwestern and northeastern) forest stands.

### Fire exposure variation among HVRA classes and within patches

Box plots showing the dispersal of BP, CFL and FS output values among the HVRA classes illustrate a large range of variability (Fig. 11). Average BP values for the 27 HVRA classes ranged from a minimum of  $BP = 0.2 \cdot 10^{-2}$  for the few authorized dumpsites (AD) in isolated areas to a maximum of  $BP = 0.7 \times 10^{-1}$  for the livestock farms (FA) in valley bottom open areas surrounded by fast-fire-spreading light fuels. The BP results highlighted several structures/patches of some HVRA classes (power lines (PL), rural housing (RH), grazed pastures (GP) and

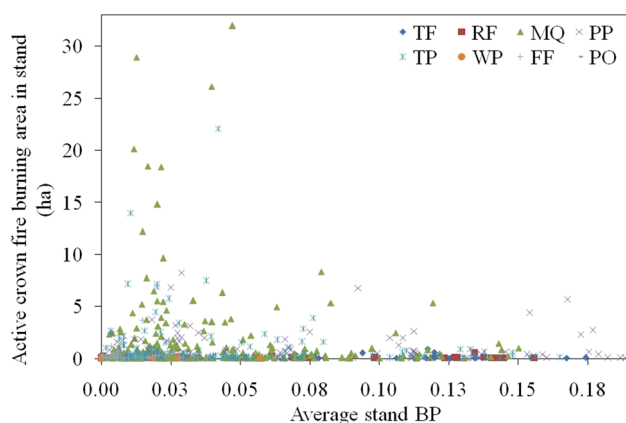


**Fig. 10** Scatter plot of the stand patches (from forest-type fuel models) burning with active crown fire versus the average burn probability. TF: thicket-stage forests; RF: riparian forest; MQ: Mediterranean *Quercus* spp. forests; PP: pole-stage *Pinus* spp. plantations; TP: timber-stage *Pinus* spp. plantations; WP: wooded pastures; FF: *Fagus sylvatica* forests; PO: *Populus* spp. plantations

firewood forests (FF), in particular; Fig. 11) with very high fire likelihood values (dots) above the 90th percentile (upper whisker limits in the respective HVRA box plots), and even above the 97th percentile for all HRVAs (BP > 0.155, Fig. 11). With regard to the fire intensity outputs summarized through the CFL box plots (Fig. 11), commercial pine timber afforestations (PI) showed the most hazardous conditions, with 90th percentile FL values of over 6.5 m for stands predominantly burning under fast-fire-front-spreading conditions. Other HVRA classes (i.e., FF, RH and PL) also showed high intensity values above the 97th percentile for all HRVAs (CFL = 3.75 m, Fig. 11) in certain structures/patches covered by high-fuel-load areas. Industrial buildings (IN), medio-European beech forests (MB) and mining sites (MS) presented the lowest average values, below the 25th percentile for all HVRA classes (CFL = 1.07 m, Fig. 11b). Mediterranean thermophilous scree (TS), sclerophyllous forests (SQ) and *J. communis* scrub on calcareous grasslands (JS) showed the highest average FS values (FS > 2400 ha; Fig. 11), which were almost twice the average value for all HVRA classes (FS = 1290 ha), although several other HVRA classes such as livestock farms (FA), churches and hermitages (CH) and seminatural dry grasslands (SG) also broadly surpassed the average HVRA value (Fig. 11). Some other classes like rural housing (RH) and firewood forests (FF) exhibited extreme outlying values within classes (dots), above the 97th percentile for all HVRA classes (FS = 3776 ha, Fig. 11).

Scatter plots of the average BP, CFL and FS values for individual HVRA patches revealed important variations among and within the different classes (Fig. 12). In general terms, most HVRA classes showed a decreasing point cloud concentration pattern from the lowest average BP

and CFL values (BP < 0.05 and CFL < 2 m) to moderate-high BP (0.10 < BP < 0.15) and moderate average CFL (2 m < CFL < 4 m) values (e.g., FA, FF, GP, PL or RH; Fig. 12). However, it is difficult to describe any pattern for those HVRA classes with a small number of patches or sites (<15, Table 2; e.g., AF, CS or CV, Fig. 12). With regard to FS, for HVRA classes with many patches (>500; RH, PL, PI, FF and GP; Table 2), the highest values (FS > 3200 ha; Fig. 12) are clustered at moderate-high BP (0.04 < BP < 0.12; Fig. 12). The *Pinus* spp. commercial afforestation (PI; Fig. 12) showed the most scattered point cloud, and many patches presented high overall wildfire exposure, with values above the 97th percentile for BP or CFL (BP > 0.155; CFL > 3.75 m; Figs. 11 and 12) and also above the 97th percentile for FS (FS > 3776 ha; Figs. 11, 12).

## Discussion

We used a fire spread simulation approach to analyze HVRA wildfire exposure in a forest-rural-urban intermix area located in northern Spain. Although the modeling outcomes are taken from a relatively small area (28,000 ha), there are many Mediterranean northern-rim regions, especially in Europe (e.g., all of the pre-Pyrenees and inland mountainous areas in Spain), with similar landscape configuration in terms of topography and vegetation, weather conditions and anthropic activities. Other studies in Mediterranean northern-rim areas (e.g., in southern France and central-northern Italy) with different land cover and landscape management practices could help us to better understand local wildfire exposure variation according to HVRA classes. In this study, we also analyzed indexes related to large fire initiation and fire spread within the study area, which, in combination with the assessment of HVRA fire exposure, can help fire managers to address fire risk management and policy making in a more informed way. Until now, only very few studies in southern Europe have considered large fire spread for a realistic fire likelihood estimation (Salis et al. 2013; Kalabokidis et al. 2013), yet large fires are known to be responsible for most of the burned area in Mediterranean climate areas. Similarly, since fire intensity is strongly related to spread direction (e.g., heading, flanking and backing), large fire modeling is important in intensity estimation weighted by burning probability and, by extension, in fire hazard estimates (Miller and Ager 2013).

Fire occurrence analysis in Mediterranean areas is a prerequisite for fire modeling, since most fires are associated with anthropic activities (Martínez et al. 2009; Padilla and Vega-García 2011; Ager et al. 2014b; e.g., lightning caused just ~2 % fires in the study area) and exhibit

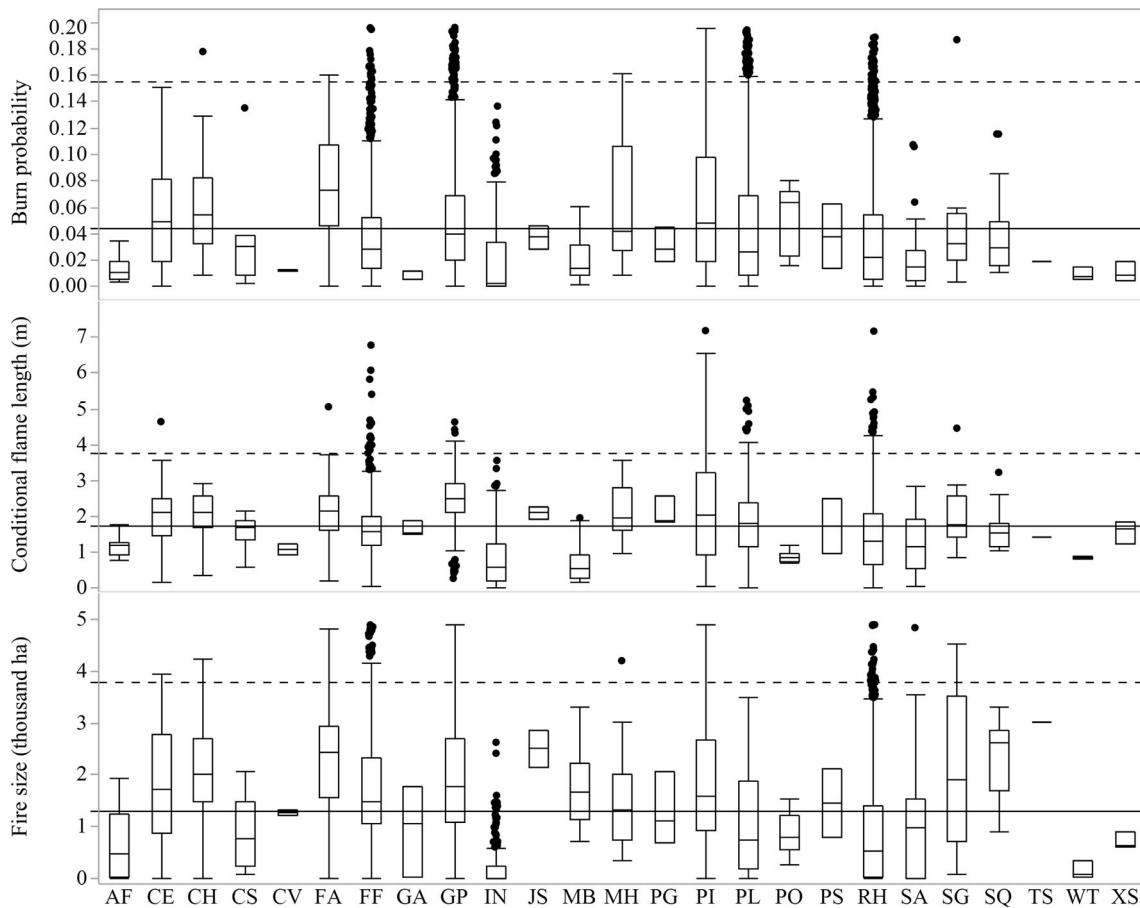


**Fig. 11** Box plots of burn probability (BP), conditional flame length (CFL) and fire size (FS) for the highly valued resources and assets in the study area (see Table 2 for abbreviations). The *box* indicates the first/third quartiles, the *whiskers* indicate the 10th/90th percentiles, the *black line within the box* is the median, and the *dots* correspond to

values below the 10th percentile or above the 90th percentile. The *horizontal continuous lines* indicate the average value (BP = 0.0437; CFL = 1.74 m; FS =  $1.29 \times 10^3$  ha) and the *discontinuous lines* the 97th percentile value (BP = 0.155; CFL = 3.75 m; FS =  $3.77 \times 10^3$  ha)

spatial–temporal ignition patterns that must be taken into account for accurate fire modeling (Bar-Massada et al. 2011; Salis et al. 2014, 2015). The anthropic causes of fire ignition are often unknown (45 % in the study area; Fig. 3c); however, it is expected they keep the same proportionality found in known cause fires. Further research to integrate spatial–temporal wildfire occurrence and causality models with fire spread and behavior simulation approaches would lead to a better understanding of spatial burn patterns (Bar-Massada et al. 2011) and historical changes in fire likelihood in the Mediterranean basin. More research is also needed to assess the potential for preventing human-caused fires and reducing the probability of landscape burning (e.g., efforts focused on reducing fires from well-known causes such as grain-harvesting machinery).

Fire modeling input data and the spatial identification of HVRA are becoming considerably more accurate, reducing the uncertainty and possible sources of error in fire modeling and fire risk assessment. High-resolution data on

local topography (5 m) and spatially explicit canopy characteristics derived from low-density airborne LiDAR ( $0.5$  first returns  $m^{-2}$ ), coupled with accurate land use/land cover information (e.g., 1:5000 SIGPAC map), have enabled landscape information input data to be characterized at fine scales (20 m). In addition, the EGIF fire database (MAGRAMA 2014) now contains complete records for more than 20 years covering most of Spain, providing extensive information on spatial ignition patterns and the associated fire causality. With regard to local wind speed and direction input data, surface wind fields can now be generated at fine resolutions (e.g.,  $<150$  m) through models (WindNinja; Forthofer et al. 2014a, b) using weather station records, which can be used to increase the accuracy of fire modeling outcomes. Once a pixel-based causative factor maps have been compiled, geospatial HVRA data (e.g., from the land registry, IDENA and IGN) provide sufficient detail to assess wildfire exposure at the level of individual structures.

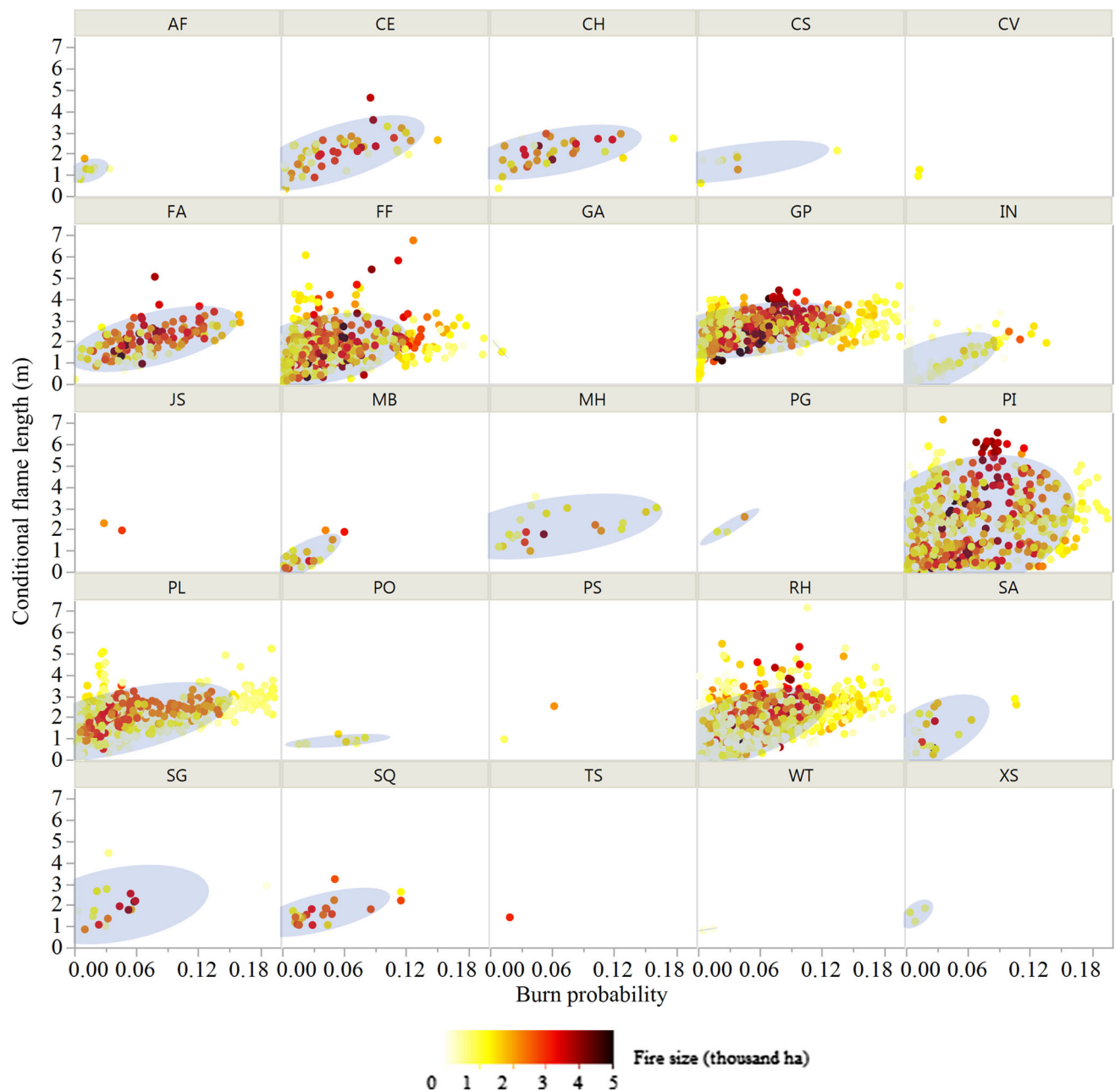


**Fig. 12** HVRA average conditional flame length versus average burn probability scatter plots. Each point represents a patch/site for a HVRA (see Table 2 for abbreviations) and is colored according to the

average fire size. The shaded area shows the bivariate normal density ellipse containing 90 % of the patches

Fire spread and behavior modeling outcomes permitted to identify areas and HVRA (Fig. 12) where there is need to implement and prioritize fuel treatments and mitigate expected potential losses from large wildfires. The awareness of the role played by efficient fire management programs in central Navarra increased after the 2009 forest-rural intermix fires, which promoted the undertaking of strategically placed fuel treatments. Those treatments were spatially located based on expert criteria (i.e., ravine junctions and crest junctions; Costa et al. 2011) usually in conifer

afforestation and consisted in the underburn after commercial thinning. In broadleaf natural forests, the treatments mostly consisted in the suppressed and dominated tree firewood cuts. Nonetheless, the expert criteria could be conditioned by the lack of experience (few observed large fires that in the future might be ignited elsewhere or spread under different weather conditions), and the limited budgets and personnel do not allow implementing the desired fuel treatments for the entire landscape. Within this context, our methodology accounts for the most likely environmental



conditions that can lead to large wildfires in the study area, and takes into account historically based ignited pattern. Moreover, our approach allows to quantify and map fine-scale fire likelihood (Fig. 6a), intensity (Fig. 6b), large fire sources (Fig. 8a) and ember-emitting forest stands (Fig. 8b), and thus to transfer to land managers more awareness and knowledge about fire behavior and exposure nearby resources and assets.

The results suggest that BP outputs for our study area were strongly influenced by the frequent NW-N wind direction and the fast-burning fuel models that played a key role in surface fire spread, as shown in the areas with the highest BP values. This was primarily related to the spread of several large fires from the northern parts of the study area through cereal crops and herbaceous fuel types. Continuous non-burnable features (i.e., motorways, railways and rivers) in flat areas mainly covered by light fuels were sufficient to contain surface fire spread, as shown in sharp BP transitions. Nevertheless, we should not overlook the influence of spotting on large fire propagation and, by extension, on BP, as recent extreme fire events in the study area (e.g., Iza-gaondoa 2009 fire with 300 m spotting distance; Bomberos de Navarra pers. comm.) have shown that the heading fire intensity may be sufficient to overcome the non-burnable barriers to surface fire spread. The highest intensities (CFL > 2.4 m; Fig. 6b) were found in steep-sloped areas when aligned with the dominant wind direction in high-fuel-load models (i.e., thicket-stage forests and shrublands). The shrubby pastures that often surround urban areas must be considered a potential source of damage to HVRAs, since their average burning intensities (CFL > 2.5 m; Table 3) exceed the direct attack capabilities of firefighting crews (Andrews et al. 2011). In the study area, FS results revealed that three-quarters of fires would spread in excess of 750 ha (Fig. 7) under extreme weather conditions in the absence of suppression efforts; fortunately, no fire of this size has been observed to date. There are three possible explanations: (1) the rapid-response first attack, due to the proximity of automatic dispatch crews; (2) the efficient fire containment by ground crews and machinery, facilitated by the high road density and the ease of access to agricultural and forest lands (Fig. 5); and (3) the very limited number of fire ignitions under extreme weather conditions until now. Even so, FPI results revealed areas with large fire potential (Fig. 8a) where ignition prevention efforts need to be intensified, as they are the ignition sites of the most recent large fire events (Fig. 1). The largest fire source areas relative to burning frequency are mainly forested north-facing slopes in the northern parts of the study area (high SSR; Fig. 8b), where fire impacts are caused by fires ignited in the vicinity. Conversely, the most relevant sink areas (low SSR; Fig. 8b) are located on the boundaries of urban areas in the central part of the study area. The SSR revealed fire-prone forested

areas in the mountains of the central part of the study area (SSR < 2; e.g., the whole of the San Cristobal mountain), which is consistent with the observed fire events in these areas that spread from fires ignited in urban areas and roads.

Major wildfire exposure differences were observed between HVRAs, as shown in the scatter plots (Fig. 12). This information could be very useful for landscape managers in prioritizing fuel treatments for hazardous vegetation surrounding high relative importance structures, like residential housing (RH) and industrial buildings (IN) (Ager et al. 2012; Alcasena et al. 2015). Moreover, although further detailed studies would be needed, reducing hazardous vegetation in housing vicinities—at least in the 60 m buffer HIZ (Cohen 2008)—would in theory create safe confinement areas in the event a wildfire, due to the low flammability of the materials used in the local constructions, the low probability of ember ignition (urban areas are surrounded by agricultural lands and far from active crown fire areas) and the improved fire suppression capabilities of ground crews. The current fire confinement capacity achieved through investment in linear non-burnable infrastructure (e.g., highways) for flat areas with herbaceous fuel models in the southern part of the study area suggests that further investment should be made part of the strategic fuel management containment strategy to facilitate fire suppression in these locations (Ager et al. 2013). Although major highways in the study area could become a good opportunities for fire suppression, they usually present strips with low vegetation and dense bushy barriers in the maintenance zone. In these cases, it would be advisable to widen the low-vegetation areas (i.e., maintaining short herbaceous grass vegetation), and to thin and prune as much as possible the bushy barriers, as well as to prefer low-flammability species and to remove the accumulated dead materials. The benefits of the management of fuels in the vicinity of major highways can be tested and quantified by applying fire spread modeling, to determine the best strategy as well as the potential to suppress wildfires.

We spatially identified in the ACP map (Fig. 9b), and even at stand level (Fig. 10), the areas in which mitigation should be prioritized to disable the spotting fires that easily overwhelmed extinction capabilities in past fires. Those areas are mainly located in hilly terrain and rough mountain windward edge crests, where dominant winds and slope are aligned with the heading fire major runs (Costa et al. 2011): Here the transition from surface to active crown fires is fast under extreme weather conditions. The initiation of the crown-to-crown transmission can be avoided elevating the canopy base height or disrupting crown continuity within stands. The typical forest stands usually correspond to overstocked pole-stage *Pinus nigra* afforestation (Table 5), characterized by a very low canopy

**Table 5** Summary of the forest vegetation types (Fig. 2) in the study area and expected area burned by active crown fires (ACF; Fig. 9a)

Forest vegetation types (abbreviation)	Number of stands	Average stand area (ha)	Total area (ha)	Percentage of active crown fires (%)
Thicket-stage forest (TF)	436	1.2	527.9	1.0
Riparian forest (RF)	246	0.6	145.2	3.0
Mediterranean <i>Quercus</i> ssp. forest (MQ)	1786	2.9	5163.1	7.7
Pole-stage <i>Pinus nigra</i> plantations (PP)	230	3.3	758.0	13.6
Timber-stage <i>Pinus nigra</i> plantations (TP)	232	8.1	1878.6	7.5
Wooded pastures (WP)	269	1.0	260.2	0.1
<i>Fagus sylvatica</i> forests (FF)	67	22.7	1523.1	1.1
<i>Populus</i> ssp. plantations (PO)	14	1.7	24.2	3.0

base height (dead branches at ground level and shrubby ladder fuels in the understory), high canopy bulk density (afforestation with 2500 trees ha<sup>-1</sup>) and high canopy cover. Overall, mitigation measures would therefore combine heavy weight thinning, pruning up to 2–2.5 m (at a maximum height of one-third of tree height), slash and laddered fuel underburn, and beef livestock extensive grazing to control the growth of heliophilous shrubs (e.g., *Rubus* sp. and *Rosa canina*) in the understory. The effectiveness of the abovementioned fire risk mitigation strategies can be evaluated and quantified using fire spread modeling, in order to identify the best compromise among risk reduction, costs and environmental constraints. Work is in progress to assess, applying a burn probability approach, the trade-offs among competing fuel management strategies for fire risk mitigation purposes within the study area as well as in other Mediterranean ecosystems.

## Conclusions

We presented a consistent methodological framework for exposure analysis that could be adopted as the preliminary step in fire risk mapping and mitigation for land managers and policy makers. In this case study, we followed a stochastic fire modeling approach based on a robust quantitative geospatial assessment framework, broadly used and accepted in the USA but not yet in Europe. The outputs have the potential to address the real requirements of landscape managers working with restricted budgets, who need reliable fine-scale analysis to prioritize mitigation measures, prevent and monitor fires caused by anthropic activities and define policies. Further research into the effects of fire on HVRAs coupled with the use of likelihood and intensity maps would allow a better understanding of the expected losses or benefits associated with wildfire events.

**Acknowledgments** The authors would like to thank the Forest Service of Navarra and the Fire Service of Navarra for their

participation in this study. We would also like to thank to the Area of Defense against Forest Fires (ADIF) and the State Meteorological Agency (AEMET) of the Spanish Ministry of Agriculture, Food and the Environment, as well as the Cartography Section, Department of Development of the Autonomous Government of Navarra for providing input data. This work was funded by a University of Lleida Research training fellowship to Fermín J. Alcasena Urdíroz, and by the project “Modeling approach to evaluate fire risk and mitigation planning actions” (P.O.R. SARDEGNA F.S.E. 2007-2013, Asse IV Capitale umano, Linea di Attività 1.3.1). This research article has received a grant for its linguistic revision from the Language Institute of the University of Lleida (2015 call).

**Open Access** This article is distributed under the terms of the Creative Commons Attribution 4.0 International License (<http://creativecommons.org/licenses/by/4.0/>), which permits unrestricted use, distribution, and reproduction in any medium, provided you give appropriate credit to the original author(s) and the source, provide a link to the Creative Commons license, and indicate if changes were made.

## References

- Ager AA, Finney MA, Kerns BK, Maffei H (2007) Modeling wildfire risk to northern spotted owl (*Strix occidentalis caurina*) habitat in Central Oregon, USA. For Ecol Manag 246:45–56. doi:10.1016/j.foreco.2007.03.070
- Ager AA, Vaillant NM, Finney MA (2010a) A comparison of landscape fuel treatment strategies to mitigate wildland fire risk in the urban interface and preserve old forest structure. For Ecol Manag 259(8):1556–1570. doi:10.1016/j.foreco.2010.01.032
- Ager AA, Finney MA, McMahan A, Cathcart J (2010b) Measuring the effect of fuel treatments on forest carbon using landscape risk analysis. Nat Hazards Earth Syst Sci 10:2515–2526. doi:10.5194/nhess-10-2515-2010
- Ager AA, Vaillant N, Finney MA (2011) Integrating fire behavior models and geospatial analysis for wildland fire risk assessment and fuel management planning. J Combust. doi:10.1155/2011/572452
- Ager AA, Vaillant NM, Finney MA, Preisler HK (2012) Analyzing wildfire exposure and source-sink relationships on a fire prone forest landscape. For Ecol Manag 267:271–283. doi:10.1016/j.foreco.2011.11.021
- Ager AA, Buonopane M, Reger A, Finney MA (2013) Wildfire exposure analysis on the national forests in the Pacific Northwest, USA. Risk Anal 33(6):1000–1020. doi:10.1111/j.1539-6924.2012.01911.x

- Ager AA, Day MA, McHugh CW, Short K, Gilbertson-Day J, Finney MA, Calkin DE (2014a) Wildfire exposure and fuel management on western US national forests. *Environ Manag* 145:54–70. doi:[10.1016/j.jenvman.2014.05.035](https://doi.org/10.1016/j.jenvman.2014.05.035)
- Ager AA, Preisler HK, Arca B, Spano D, Salis M (2014b) Wildfire risk estimation in the Mediterranean area. *Environmetrics* 25:384–396. doi:[10.1002/env.2269](https://doi.org/10.1002/env.2269)
- Alcasena FJ, Salis M, Ager AA, Arca B, Molina D, Spano D (2015) Assessing landscape scale wildfire exposure for highly valued resources in a Mediterranean area. *Environ Manag* 55:1200–1216. doi:[10.1007/s00267-015-0448-6](https://doi.org/10.1007/s00267-015-0448-6)
- Andersen EH, Mc Gaughey JR, Reutebuch ES (2005) Estimating forest canopy fuel parameters using LIDAR data. *Remote Sens Environ* 94(4):441–449. doi:[10.1016/j.rse.2004.10.013](https://doi.org/10.1016/j.rse.2004.10.013)
- Andrews PL, Heinsch FA, Schelvan L (2011) How to generate and interpret fire characteristics charts for surface and crown fire behavior. General Technical Report RMRS-GTR-253. USDA Forest Service, Rocky Mountain Research Station, Fort Collins
- Arca B, Duce P, Laconi M, Pellizzaro G, Salis M, Spano D (2007) Evaluation of FARSITE simulator in Mediterranean maquis. *Int J Wildl Fire* 16:563–572. doi:[10.1071/wf06070](https://doi.org/10.1071/wf06070)
- Arca B, Pellizzaro G, Duce P, Salis M, Bacciu V, Spano D, Ager A, Finney MA, Scoccimarro E (2012) Potential changes in fire probability and severity under climate change scenarios in Mediterranean areas. In: Spano D, Bacciu V, Salis M, Sirca C (eds) *Modelling fire behavior and risk*. Nuova Stampa Color Publishers, Muros, pp 92–98
- Arroyo LA, Pascual C, Manzanera JA (2008) Fire models and methods to map fuel types: the role of remote sensing. *For Ecol Manag* 256:1239–1252. doi:[10.1016/j.foreco.2008.06.048](https://doi.org/10.1016/j.foreco.2008.06.048)
- Bar-Massada A, Syphard AD, Hawbaker TJ, Stewart SI, Radeloff VC (2011) Effects of ignition location models on the burn patterns of simulated wildfires. *Environ Model Softw* 26(5):583–592. doi:[10.1016/j.envsoft.2010.11.016](https://doi.org/10.1016/j.envsoft.2010.11.016)
- Byram GM (1959) Combustion of forest fuels. In: Davis KP (ed) *Forest fire: control and use*. McGraw-Hill, New York, pp 61–89
- Calkin DE, Ager AA, Thompson MP (2011) A comparative risk assessment framework for wildland fire management: the 2010 cohesive strategy science report. General Technical Report RMRS-GTR-262. USDA Forest Service, Rocky Mountain Research Station, Fort Collins
- Cardil A, Molina DM, Ramirez J, Vega-García C (2013a) Trends in adverse weather patterns and large wildland fires in Aragón (NE Spain) from 1978 to 2010. *Nat Hazards Earth Syst Sci* 13:1393–1399. doi:[10.5194/nhess-13-1393-2013](https://doi.org/10.5194/nhess-13-1393-2013)
- Cardil A, Salis M, Spano D, Delogu G, Molina DM (2013b) Large wildland fires and extreme temperatures in Sardinia (Italy). *Iforest* 7:162–169. doi:[10.3832/ifor1090-007](https://doi.org/10.3832/ifor1090-007)
- Chung W, Jones G, Krueger K, Bramel J, Contreras M (2013) Optimising fuel treatments over time and space. *Int J Wildl Fire* 22:1118–1133. doi:[10.1071/wf12138](https://doi.org/10.1071/wf12138)
- Chuvieco E, Yebra M, Jurdao S, Aguado I, Salas FJ, García M, Nieto H, De Santis A, Cocero D, Riaño D, Martínez S, Zapico E, Recondo C, Martínez-Vega J, Martín MP, Riva J, Pérez F, Rodríguez-Silva F (2011) Field fuel moisture measurements on Spanish study sites. Department of Geography, University of Alcalá, Madrid
- Cochrane MA, Moran CJ, Wimberly MC, Baer AD, Finney MA, Beckendorf KL, Eidenshink J, Zhu Z (2012) Estimation of wildfire size and risk changes due to fuels treatments. *Int J Wildl Fire* 21:357–367. doi:[10.1071/wf11079](https://doi.org/10.1071/wf11079)
- Cohen J (2008) The wildland–urban interface fire problem forest history today: a consequence of the fire exclusion paradigm. *For History Today* (Fall) 20–26. [http://www.fs.fed.us/rm/pubs\\_other/rmrs\\_2008\\_cohen\\_j002.pdf](http://www.fs.fed.us/rm/pubs_other/rmrs_2008_cohen_j002.pdf). Accessed 24 Apr 2015
- Conalgtton RG, Green K (1999) *Assessing the accuracy of remotely sensing data: Principles and practices*. Lewis Publishers, Boca Raton
- Costa P, Castellnou M, Larrañaga A, Miralles M, Kraus PD (2011) Prevention of large wildfires using the fire types concept. Unitat Tècnica del GRAF, Divisió de Grups Operatius Especials. Direcció General de Prevenció, Extinció d'Incendis i Salvaments. Departament d'Interior. ISBN: 978-84-694-1457-6. Generalitat de Catalunya, Barcelona. [http://www.efi.int/files/attachments/publicacions/handbook-prevention-large-fires\\_en.pdf](http://www.efi.int/files/attachments/publicacions/handbook-prevention-large-fires_en.pdf). Accessed 20 Aug 2015
- Erdody TL, Moskal LM (2010) Fusion of LiDAR and imagery for estimating forest canopy fuels. *Remote Sens Environ* 114:725–737. doi:[10.1016/j.rse.2009.11.002](https://doi.org/10.1016/j.rse.2009.11.002)
- Fallowski MJ, Gessler PE, Morgan P, Hudak AT, Smith AMS (2005) Characterizing and mapping forest fire fuels using Aster imagery and gradient modeling. *For Ecol Manag* 217:2–3. doi:[10.1016/j.foreco.2005.06.013](https://doi.org/10.1016/j.foreco.2005.06.013)
- Fernandes P (2009) Examining fuel treatment longevity through experimental and simulated surface fire behaviour: a maritime pine case study. *Can J For Res* 39:2529–2535. doi:[10.1139/X09-145](https://doi.org/10.1139/X09-145)
- Fernandes PM, Davies GM, Ascoli D, Fernández C, Moreira F, Rigolot E, Stoof CR, Vega JA, Molina D (2013) Prescribed burning in southern Europe: developing fire management in a dynamic landscape. *Front Ecol Environ* 11:e4–e14. doi:[10.1890/120298](https://doi.org/10.1890/120298)
- Finney MA (2002) Fire growth using minimum travel time methods. *Can J For Res* 32(8):1420–1424. doi:[10.1139/x02-068](https://doi.org/10.1139/x02-068)
- Finney MA (2005) The challenge of quantitative risk analysis for wildland fire. *Fire Ecol Manag* 211:97–108. doi:[10.1016/j.foreco.2005.02.010](https://doi.org/10.1016/j.foreco.2005.02.010)
- Finney MA (2006) An overview of FlamMap fire modeling capabilities. In: Andrews PL, Butler BW (eds) *Fuels management—how to measure success*. USDA Forest Service, Rocky Mountain Research Station, Fort Collins, pp 213–220
- Finney MA (2007) A computational method for optimising fuel treatment locations. *Int J Wildl Fire* 16:702–711. doi:[10.1071/wf06063](https://doi.org/10.1071/wf06063)
- Finney MA, Seli RC, McHugh CW, Ager AA, Bahro B, Agee JK (2007) Simulation of long-term landscape-level fuel treatment effects on large wildfires. *Int J Wildl Fire* 16:712–727. doi:[10.1071/wf06064](https://doi.org/10.1071/wf06064)
- Forthofer J, Butler B (2007) Differences in simulated fire spread over Askervein Hill using two advanced wind models and a traditional uniform wind field. In: Butler BW, Cook W (eds) *The fire environment-innovations, management, and policy; conference proceedings*. US Department of Agriculture, Forest Service, Rocky Mountain Research Station, Fort Collins, pp 26–30
- Forthofer JM, Butler BW, Wagenbrenner NS (2014a) A comparison of three approaches for simulating fine-scale surface winds in support of wildland fire management. Part I. Model formulation and comparison against measurements. *Int J Wildl Fire* 23:969–981. doi:[10.1071/wf12089](https://doi.org/10.1071/wf12089)
- Forthofer JM, Butler BW, Mc Hugh CW, Finney MA, Bradshaw LS, Stratton RD, Shannon KS, Wagenbrenner NS (2014b) A comparison of three approaches for simulating fine-scale surface winds in support of wildland fire management. Part II. An exploratory study of the effect of simulated winds on fire growth simulations. *Int J Wildl Fire* 23:982–994. doi:[10.1071/wf12090](https://doi.org/10.1071/wf12090)
- Fulé PZ, Ribas M, Gutiérrez E, Vallejo R, Kaye MW (2008) Forest structure and fire history in an old *Pinus nigra* forest, eastern Spain. *For Ecol Manag* 255:1234–1242. doi:[10.1016/j.foreco.2007.10.046](https://doi.org/10.1016/j.foreco.2007.10.046)
- Ganteaume A, Camia A, Jappiot M, San-Miguel-Ayanz J, Long-Fournel M, Lampin C (2013) A review of the main driving

- factors of forest fire ignition over Europe. *Environ Manag* 51(3):651–662. doi:10.1007/s00267-012-9961-z
- Gao X, Giorgi F (2008) Increased aridity in the Mediterranean region under greenhouse gas forcing estimated from high resolution regional climate projections. *Glob Planet Change* 62(3–4):195–209. doi:10.1016/j.gloplacha.2008.02.002
- García M, Riaño D, Chuvieco E, Salas F, Danson FM (2011) Multispectral and LiDAR data fusion for fuel type mapping using Support Vector Machine and decision rules. *Remote Sens Environ* 115:1369–1379. doi:10.1016/j.rse.2011.01.017
- Giannakopoulos C, Le Sager P, Bindi M, Moriondo M, Kostopoulou E, Goodess CM (2009) Climatic changes and associated impacts in the Mediterranean resulting from a 2 °C global warming. *Glob Planet Change* 68:209–224. doi:10.1016/j.gloplacha.2009.06.001
- Giorgi F, Lionello P (2008) Climate change projections for the Mediterranean region. *Glob Clim Change* 63:90–104. doi:10.1016/j.gloplacha.2007.09.005
- Gobierno de Navarra (2014a) SIGPAC Navarra, Sistema de Información Geográfica de Navarra para la Política Agraria Comunitaria. <http://sigpac.navarra.es>. Accessed 24 Apr 2015
- Gobierno de Navarra (2014b) IDENA, Infraestructura de Datos Espaciales de Navarra. <http://idena.navarra.es>. Accessed 24 Apr 2015
- Gobierno de Navarra (2014c) Ministry of Public Works, Transport and Housing in the Government of Navarra, Pamplona
- González-Ferreiro E, Diéguez-Aranda U, Crecente-Campo F, Barreiro-Fernández L, Miranda D, Castedo-Dorado F (2014) Modelling canopy fuel variables for *Pinus radiata* D. Don in NW Spain with low-density LiDAR data. *Int J Wildl Fire* 23:350–362. doi:10.1071/wf13054
- Gonzalez-Olabarria JR, Rodriguez F, Fernandez-Landa A, Mola-Yudego B (2012a) Mapping fire risk in the Model Forest of Urbión based on airborne LiDAR measurements. *For Ecol Manag* 282:149–156. doi:10.1016/j.foreco.2012.06.056
- Gonzalez-Olabarria JR, Brotons L, Gritten D, Tudela A, Teres JAI (2012b) Identifying location and causality of fire ignition hotspots in a Mediterranean region. *Int J Wildl Fire* 21:905–914. doi:10.1071/wf11039
- Haas JR, Calkin DE, Thompson MP (2013) A national approach for integrating wildfire simulation modeling into Wildland Urban Interface risk assessments within the United States. *Landsc Urban Plan* 119:44–53. doi:10.1016/j.landurbplan.2013.06.011
- Hermosilla T, Ruiz LA, Kazakova AN, Coops NC, Moskal LM (2014) Estimation of forest structure and canopy fuel parameters from small-footprint full-waveform LiDAR data. *Int J Wildl Fire* 23:224–233. doi:10.1071/wf13086
- IPCC (2014) Climate change 2014: mitigation of climate change. In: Edenhofer O, Pichs-Madruga R, Sokona Y, Farahani E, Kadner S, Seyboth K, Adler A, Baum I, Brunner S, Eickemeier P, Kriemann B, Savolainen J, Schlömer S, Von Stechow C, Zwickel T, Minx JC (eds) Contribution of working group III to the fifth assessment report of the intergovernmental panel on climate change. Cambridge University Press, Cambridge
- Kalabokidis K, Palaiologou P, Finney M (2013) Fire Behavior Simulation in Mediterranean Forests Using the Minimum Travel Time Algorithm. In: International Association of Wildland Fire (eds) Proceedings of 4th fire behavior and fuels conference. International Association of Wildland Fire, St. Petersburg, pp 468–492
- Koo E, Pagni PJ, Weise DR, Woycheese JP (2010) Firebrands and spotting ignition in large-scale fires. *Int J Wildl Fire* 19:818–843. doi:10.1071/wf07119
- Legendre P, Legendre L (1998) Numerical ecology. 2nd edn. Elsevier, Amsterdam
- Lloret F, Calvo E, Pons X, Díaz-Delgado R (2002) Wildfires and landscape patterns in the Eastern Iberian Peninsula. *Landsc Ecol* 17:745–759
- Loepfe L, Martinez-Vilalta J, Oliveres J, Pinol J, Lloret F (2010) Feedbacks between fuel reduction and landscape homogenization determine fire regimes in three Mediterranean areas. *For Ecol Manag* 259:2366–2374. doi:10.1016/j.foreco.2010.03.009
- MAGRAMA (2014) Ministerio de Agricultura, Alimentación y Medio Ambiente, Forest Fires database in Spain, Area of Defense Against Forest Fires, Madrid
- Martínez J, Vega-García C, Chuvieco E (2009) Human-caused wildfire risk rating for prevention planning in Spain. *J Environ Manag* 90:1241–1252. doi:10.1016/j.envman.2008.07.005
- Mc Gaughey R (2014) FUSION/LDV: Software for lidar data analysis and visualization. Version 3.41. US Department of Agriculture, Forest Service, Pacific Northwest Research Station, Seattle
- Miller C, Ager AA (2013) A review of recent advances in risk analysis for wildfire management. *Int J Wildl Fire* 22:1–14. doi:10.1071/wf11114
- Ministerio de Fomento (2010) Plan Nacional de Ortofotografía aérea. Especificaciones Técnicas para vuelo fotogramétrico digital con vuelo LiDAR. Ministerio de Fomento, Madrid. <http://www.ign.es/PNOA>. Accessed 24 Apr 2013
- Mitsopoulos I, Mallinis G, Arianoutsou M (2014) Wildfire risk assessment in a typical Mediterranean wildland–urban interface of Greece. *Environ Manag*. doi:10.1007/s00267-014-0432-6
- Molina D, Castellnou M, García-Marco D, Salgueiro A (2010) Improving fire management success through fire behaviour specialists. In: Sande J, Rego F, Fernandes P, Rigolot E (eds) Towards integrated fire management-outcomes of the European Project Fire Paradox. European Forest Institute, Joensuu, pp 105–119
- Moreira F, Viedma O, Arianoutsou M, Curt T, Koutsias N, Rigolot F, Barbati A, Corona P, Vaz P, Xanthopoulos G, Mouillot F, Bilgili E (2011) Landscape–wildfire interactions in southern Europe: implications for landscape management. *J Environ Manag* 92:2389–2402. doi:10.1016/j.jenvman.2011.06.028
- Mouillot D, Mason NWH, Dumay O, Wilson JB (2005) Functional regularity: a neglected aspect of functional diversity. *Oecologia* 142:353–359. doi:10.1007/s00442-004-1744-7
- Mutlu M, Popescu SC, Zhao K (2008) Sensitivity analysis of fire behavior modeling with LIDAR derived surface fuel maps. *For Ecol Manag* 256:289–294. doi:10.1016/j.foreco.2008.04.014
- Padilla M, Vega-García C (2011) On the comparative importance of fire danger rating indices and their integration with spatial and temporal variables for predicting daily human-caused fire occurrences in Spain. *Int J Wildl Fire* 20:46–58. doi:10.1071/wf09139
- Pal JS, Giorgi F, Bi X (2004) Consistency of recent European summer precipitation trends and extremes with future regional climate projections. *Geophys Res Lett* 31:L13202. doi:10.1029/2004gl019836
- Pausas JG, Bladé C, Valdecantos A, Seva JP, Fuentes D, Alloza JA, Vilagros A, Bautista S, Cortina J, Vallejo R (2004) Pines and oaks in the restoration of Mediterranean landscapes in Spain: new perspectives for an old practice—a review. *Plant Ecol* 171:209–220. doi:10.1023/b:vege.0000029381.63336.20
- Peralta J (2000) Sectorización fitoclimática de Navarra. Series de vegetación y sectorización fitoclimática de la comarca agraria III. Departamento de Agricultura, Ganadería y Alimentación. Gobierno de Navarra, Pamplona
- Peterson B, Nelson K (2011) Developing a regional canopy fuels assessment strategy using multi-scale LiDAR. In: J Rombouts (ed) Proceedings of SilviLaser 2011, 11th international conference on LiDAR applications for assessing forest ecosystems. Hobart, Tasmania
- Rodriguez-Aseretto RD, Boca R, San-Miguel-Ayanz J, Liberta G, Schmuck G, Camia A, Schulte E, Petroliaqkis T, Durrant T,

- Boccacci F, Di-Leo M (2014) Forest fires in Europe, Middle East and North Africa 2013. Publications Office of the European Union, Luxembourg
- Romero-Calcerrada R, Perry GLW (2004) The role of land abandonment in landscape dynamics in the SPA Encinares del río Alberche y Cofio, Central Spain, 1984–1999. *Landsc Urban Plan* 66:217–232. doi:[10.1016/s0169-2046\(03\)00112-9](https://doi.org/10.1016/s0169-2046(03)00112-9)
- Rothermel RC (1972) A mathematical model for predicting fire spread in wildland fuels. Research paper, INT-115. USDA Forest Service, Intermountain Forest and Range Experiment Station, Ogden
- Roura-Pascual N, Pons P, Etienne M, Lambert B (2005) Transformation of a rural landscape in the Eastern Pyrenees between 1953 and 2000. *Mt Res Dev* 25:252–261
- Salis M (2008) Fire behaviour simulation in Mediterranean maquis using FARSITE (fire area simulator). PhD thesis. Università degli Studi di Sassari, Dipartimento di Economia e Sistemi Arborei, Sassari
- Salis M, Ager AA, Arca B, Finney MA, Bacciu V, Duce P, Spano D (2013) Assessing exposure of human and ecological values to wildfire in Sardinia, Italy. *Int J Wildl Fire* 22(4):549–565. doi:[10.1071/wf11060](https://doi.org/10.1071/wf11060)
- Salis M, Ager A, Finney M, Arca B, Spano D (2014) Analyzing spatiotemporal changes in wildfire regime and exposure across a Mediterranean fire-prone area. *Nat Hazards* 71:1389–1418. doi:[10.1007/s11069-013-0951-0](https://doi.org/10.1007/s11069-013-0951-0)
- Salis M, Ager AA, Alcasena FJ, Arca B, Finney MA, Pellizzaro G, Spano D (2015) Analyzing seasonal patterns of wildfire exposure factors in Sardinia, Italy. *Environ Monit Assess* 187:4175. doi:[10.1007/s10661-014-4175-x](https://doi.org/10.1007/s10661-014-4175-x)
- San-Miguel-Ayán J, Moreno JM, Camia A (2013) Analysis of large fires in European Mediterranean landscapes: lessons learned and perspectives. *For Ecol Manag* 294:11–22. doi:[10.1016/j.foreco.2012.10.050](https://doi.org/10.1016/j.foreco.2012.10.050)
- San-Miguel-Ayán J, Camia A (2010) Forest fires. In: EEA (European Environment Agency) (ed) Mapping the impacts of natural hazards and technological accidents in Europe: an overview of the last decade. Publications of European Union, Luxembourg. doi:[10.2800/62638](https://doi.org/10.2800/62638)
- San-Roman-Sanz A, Fernandez C, Mouillot F, Ferrat L, Istria D, Pasqualini V (2013) Longterm forest dynamics and land-use abandonment in the Mediterranean mountains, Corsica, France. *Ecol Soc* 18(2):38. doi:[10.5751/es-05556-180238](https://doi.org/10.5751/es-05556-180238)
- Scarascia-Mugnozza G, Oswald H, Piussi P, Radoglou K (2000) Forests of the Mediterranean region: gaps in knowledge and research needs. *For Ecol Manag* 132:97–109. doi:[10.1016/s0378-1127\(00\)00383-2](https://doi.org/10.1016/s0378-1127(00)00383-2)
- Scott J (2006) An analytical framework for quantifying wildland fire risk and fuel treatment benefit. In: Andrews PL, Butler BW (comps), Fuels management—how to measure success: conference proceedings. Portland, OR, March 28–30, 2006, Proceedings RMRS-P-41. USDA Forest Service, Rocky Mountain Research Station, Fort Collins, pp 169–184
- Scott JH, Burgan R (2005) Standard fire behavior fuel models: a comprehensive set for use with Rothermel's surface fire spread model. General Technical Report RMRS-GTR-153. USDA Forest Service, Rocky Mountain Research Station, Fort Collins
- Scott JH, Reinhardt ED (2001) Assessing crown fire potential by linking models of surface and crown fire behavior. Research paper RMRS-RP-29. US Department of Agriculture, Forest Service, Rocky Mountain Research Station, Fort Collins
- Scott J, Helmbrecht D, Thompson MP, Calkin DE, Marcille K (2012) Probabilistic assessment of wildfire hazard and municipal watershed exposure. *Nat Hazards* 64:707–728. doi:[10.1007/s11069-012-0265-7](https://doi.org/10.1007/s11069-012-0265-7)
- Scott JH, Thompson MP, Calkin DE (2013) A wildfire risk assessment framework for land and resource management. General Technical Reports RMRS-GTR-315. USDA Forest Service, Rocky Mountain Research Station, Fort Collins
- Thompson MP, Calkin DE, Finney MA, Ager AA, Gilbertson-Day JW (2011) Integrated national-scale assessment of wildfire risk to human and ecological values. *Stoch Environ Res Risk Assess* 25:761–780. doi:[10.1007/s00477-011-0461-0](https://doi.org/10.1007/s00477-011-0461-0)
- Thompson MP, Scott J, Helmbrecht D, Calkin DE (2012) Integrated wildfire risk assessment: framework development and application on the Lewis and Clark National Forest in Montana, USA. *Integr Environ Assess Manag* 9(2):329–342. doi:[10.1002/ieam.1365](https://doi.org/10.1002/ieam.1365)
- Thompson MP, Haas JR, Gilbertson-Day JW, Scott JH, Langowski P, Bowne E, Calkin DE (2015) Development and application of a geospatial wildfire exposure and risk calculation tool. *Environ Model Softw* 63:61–72. doi:[10.1016/j.envsoft.2014.09.018](https://doi.org/10.1016/j.envsoft.2014.09.018)
- Van Wagner CE (1977) Conditions for the start and spread of crown fire. *Can J For Res* 7(1):23–34. doi:[10.1139/x77-004](https://doi.org/10.1139/x77-004)
- Vega-García C, Chuvieco E (2006) Applying local measures of spatial heterogeneity to Landsat-TM images for predicting wildfire occurrence in Mediterranean landscapes. *Land Ecol* 21:595–605. doi:[10.1007/s10980-005-4119-5](https://doi.org/10.1007/s10980-005-4119-5)
- Werth PA, Potter BE, Clements CB, Finney MA, Goodrick SL, Alexander ME, Cruz MG, Forthofer JA, McAllister SS (2011) Synthesis of knowledge of extreme fire behavior: volume I for fire managers. General Technical Report. PNW-GTR-854. US Department of Agriculture, Forest Service, Pacific Northwest Research Station, Portland
- WWF (2006) Grandes incendios forestales, Causas y efectos de una ineficaz gestión del territorio. [http://assets.wwf.es/downloads/informe\\_incendios\\_06.pdf](http://assets.wwf.es/downloads/informe_incendios_06.pdf). Accessed 24 Apr 2015